Mestrado Integrado em Engenharia Química

Hydrogen generation from catalytic hydrolysis of sodium borohydride on a mini-reactor for portable applications

Master Thesis

by

Helder Xavier Teixeira Nunes

Developed under the curricular unit Dissertação

Performed at

CEFT – Centro de Estudos de Fenómenos de Transporte,
Faculdade de Engenharia da Universidade do Porto

Supervisor: **Alexandra Rodrigues Pinto (CEFT-DEQ)**

Co-Supervisor: **Maria Josefina Ferreira (CEFT-DEQ)**

Universidade do Porto
Faculdade de Engenharia
FEUP

Departamento de Engenharia Química

February 2014

Acknowledgements

First of all, I would like to thank to my supervisor, Dr. Alexandra Rodrigues Pinto, as well as to all members of the Centro de Estudos de Fenómenos de Transporte (CEFT), for having embraced me in the group and giving me the chance to develop my dissertation in a theme that is so appealing to me. I hope to somehow reward you with the presentation of this work!

To my co-supervisor, Eng. Josefina Ferreira, for the constant supervision and solicitude, as well as for all the scientific knowledge transmitted.

To the Laboratório Nacional de Energia e Geologia (LNEG) and to Dr. Cármen Rangel in particular, for synthesize the catalyst used in my experimental works.

To Eng. Jaime Monteiro, Eng. José Almacinha and Eng. Joaquim Fonseca, from Mechanical Engineering Department, for all the assistance provided in the construction of the reactor.

To Dr. Carlos Sá, from Electrotechnical Engineering Department, as well as to all members of the Robotics Laboratory, for the constant help in the electrotechnical problems that haunted me sporadically!

To Azemoldes, especially to designer Bruno Paiva, for all the advice provided and for helping me in the construction of the 3D design of the reactor. A special gratitude word to the Eng. Américo Nunes, not only for all the technical suggestions provided, but mostly by the wise fatherly advice and unconditional encouragement throughout life.

To Joana Madureira, classmate and lab partner, to have experienced and shared with me closely this dissertation.

To friends, from the university and childhood, by providing me so many great moments. You made this academic path unique and unforgettable.

To family, in special to my parents and my sister, for the unconditional love, dedication and support. I owe you everything.

Finally, I would like to express my deepest gratitude to Margarida Gonçalves for all availability, love and patient when I was only thinking about H_2 generation formulas. You made everything easier.

Abstract

The need to reduce greenhouse gas concentrations to sustainable levels has resulted on a demand for clean and abundant energy to substitute fossil fuels. Hydrogen (H_2) is recognized as the environmentally desirable clean fuel of the future, and it can be used directly in a proton exchange membrane (PEM) fuel cell to provide electricity to small portable applications (laptops, cell phones, iPods, iPads, etc.) with high autonomy. Chemical hydrides, in particular sodium borohydride ($NaBH_4$), present great potential to storage and generate hydrogen, through a simple catalyzed hydrolysis reaction. In this context, a novel portable batch mini-reactor (~9 cm^3) was designed with an ovoid optimized geometry, to generate and storage H_2. Most of the experiments were done with solid $NaBH_4$ and stoichiometric liquid water (alkali free) in the presence of a reused nano-particulate nickel-ruthenium based catalyst, where the following parameters were studied: $H_2O/NaBH_4$ molar ratio; catalyst/$NaBH_4$ mass ratio and temperature. Since most of the studies in this area report the H_2 production from aqueous alkaline solution of $NaBH_4$, the effect of the presence of the sodium hydroxide inhibitor was also assessed in this work.

The results revealed that increasing the parameters - $H_2O/NaBH_4$ molar ratio; catalyst/$NaBH_4$ mass ratio and temperature – enhances yield and hydrogen generation rates. With the exclusion of any excess of water (x = 0), hydrogen with 7.87 wt% (reactant only basis) was produced with an H_2 yield of 84.57%, at room temperature. Moreover, at approximately 55 ± 5°C controlled temperature, the remarkable value of 57.12 L_{H_2} min^{-1} g_{Cat}^{-1} was obtained for a $H_2O/NaBH_4$ molar ratio = 4 mol/mol. Altogether, the obtained results corroborate the efficacy of the ovoid shape reactor on hydrogen generation, comparing with a previous work, performed in a batch small reactor (≈230 cm^3) with a conical bottom geometry.

Given the crescent necessity of a green economy, generated data from this work may provide novel insights to establish a hydrogen based economy for portable applications.

Keywords: Hydrogen economy, hydrogen generation, sodium borohydride hydrolysis, Ni-Ru catalyst, reactor geometry, egg-shaped mini-reactor, PEM fuel cells.

Resumo

A necessidade de reduzir as concentrações dos gases de estufa para níveis sustentáveis tem resultado na procura de energia "limpa" e abundante capaz de substituir os combustíveis fósseis. O hidrogénio (H_2) tem surgido como um combustível economicamente desejável para o futuro, e pode ser usado diretamente numa célula combustível de eletrólito de membrana polimérica (PEM) para fornecer eletricidade para pequenos dispositivos portáteis (computadores portáteis, telemóveis, iPods, iPads, etc.) com elevada autonomia. Os hidretos químicos, em particular o borohidreto de sódio ($NaBH_4$), apresentam um elevado potencial para produzir e armazenar hidrogénio, através de uma simples reação de hidrólise catalisada. Neste contexto, desenhou-se um mini-reator portátil inovador (~9 cm^3) com uma geometria ovoide otimizada, para produzir e armazenar H_2. A maioria das experiências foram realizadas com NaBH4 sólido e uma quantidade estequiométrica de água líquida (hidrólise sem inibidor hidróxido) na presença de um catalisador nanoparticulado e reutilizado à base de níquel e ruténio, onde os seguintes parâmetros foram avaliados: rácio molar $H_2O/NaBH_4$; rácio mássico catalisador/$NaBH_4$ e temperatura. Uma vez que a maioria dos estudos já realizados nesta área descreve a produção de H_2 a partir de uma solução aquosa alcalina de $NaBH_4$, o efeito da presença do inibidor hidróxido de sódio foi também avaliado neste trabalho.

Os resultados obtidos demonstram que o aumento dos parâmetros estudados aumenta o rendimento e as taxas de produção de hidrogénio. Sem excesso de água (x = 0), foi produzido hidrogénio com uma densidade gravimétrica de 7.87 wt% (determinada com base apenas nos reagentes) com um rendimento de 84.57%, à temperatura ambiente. Além disso, obteve-se a maior taxa de reação alguma vez reportada (57.12 L_{H_2} min^{-1} g_{Cat}^{-1}) para um rácio molar $H_2O/NaBH_4$ de 4 mol/mol, a 55 ± 5ºC. De um modo geral, os resultados obtidos corroboram a eficácia da forma ovoide do reator na produção de hidrogénio.

Dada a crescente necessidade de uma economia sustentável, a informação gerada com este trabalho possui uma importância fundamental no estabelecimento de uma economia baseada no hidrogénio para aplicações portáteis.

Palavras-chave: Economia de hidrogénio, produção de hidrogénio, hidrólise do borohidreto de sódio, catalisador Ni-Ru, geometria do reator, mini-reator ovoide, células de hidrogénio tipo PEM.

Affidavit

I declare, on oath, that this work thesis is original and that all the not original contributions were appropriately referred with source identification.

Porto, 20th February 2014

_____

(Helder Xavier Teixeira Nunes)

Index of contents

Index of figures

Index of tables

Nomenclature/Glossary

A	Distance from the centre of curvature to the axis of revolution	mm
c	Constant of integration	
dP/dt	Linear region slope	bar s^{-1}
E	Activation Energy	kJ mol^{-1}
h	Thickness of the reactor	mm
K	reaction rate	mol min^{-1} g^{-1}
m_{Cat}	Catalyst mass	g
m_{H_2O}	Mass of water	g
m_{NaBH_4}	Mass of sodium borohydride	g
$m_{Sol.}$	Mass of the reactant solution	g
N_Φ	Membrane stress resultant in the meridional direction	N/mm
N_θ	Membrane stress resultant in the hoop direction	N/mm
$P_{Gas,\ Exp.}$	Absolute pressure of the gas produced	bar
$P_{Gas,\ Theo.}$	Theoretical absolute pressure of the gas	bar
R	Ideal gas constant	cm^3 bar K^{-1} mol^{-1}
r	Spherical radius	mm
R_c	Radius of curvature	mm
T	Temperature	K
V_{Cat}	Volume of catalyst	cm^3
V_{H_2O}	Water volume	cm^3
$V_{m,\ STP}$	Molar volume at STP conditions	22.466 L mol^{-1}
V_{NaBH_4}	Volume of sodium borohydride	cm^3
$V_{R,\ Fin.}$	Final volume of the reactor	cm^3

$V_{Sol.}$	Reactant solution volume	cm^3
x	Excess hydration factor	
γ	Specific weight	N/mm^3
η	Yield rate	%
σ_v	von Mises stress	N/mm^2
σ_y	Yield strength	N/mm^2
Φ	Angular coordinate	rad
Φ_0	Half-angle of opening	rad

Acronyms

AFC	Alkaline Fuel Cell	
AISI	American Iron and Steel Institute	
DMFC	Direct Methanol Fuel Cell	
DOE	Department of Energy	
EDX	Energy Dispersive X-ray	
GHSC	Gravimetric Hydrogen Storage Capacity	wt%
HGR	Hydrogen Generation Rate	$L_{H_2}\,min^{-1}\,g_{Cat}^{-1}$
MCFC	Molten Carbonate Fuel Cell	
MEA	Membrane Electrode Assembly	
PAFC	Phosphoric Acid Fuel Cell	
PEEK	Polyether Ether Ketone	
PEMFC	Proton Exchange Membrane Fuel Cell	
SEM	Scanning Electron Microscope	
SOFC	Solid Oxide Fuel Cell	
STP	Standard Temperature and Pressure	
U.S.	United States	
VHSC	Volumetric Hydrogen Storage Capacity	$kg\,m^3$
XPS	X-ray Photoelectron Spectroscopy	

1 Introduction

"Hydrogen is the most common element in the universe, and has the potential to become an inexpensive source of energy for neighbourhoods, light and heavy duty vehicles, and industry." Charlie Dent[1]

1.1 Motivation

The majority of world's man-made carbon emissions are released by the burning fossil fuels to create electricity, heat or motion. This means that it will almost certainly be impossible to reduce greenhouse gas concentrations to sustainable levels, unless large quantities of low-carbon energy can be brought on-stream to substitute for fossil fuels.

In this context, the demands for clean and abundant energy have resulted in increased attention worldwide to the possibilities of a hydrogen economy as a vision of using hydrogen as a low-carbon energy source [1].

Hydrogen is recognized as the environmentally desirable clean fuel of the future since it can be used directly in internal combustion engines or be oxidized efficiently in Polymer Electrolyte Membrane Fuel Cells (PEMFC) to provide electricity to portable applications – laptops, smart phones and iPods – with high autonomy [2]. However, in order to develop the hydrogen economy, some significant issues need to be addressed. First of all, since molecular hydrogen (H_2) does not exist in large amounts in environment to use directly as energy, it must be synthesized from other energy sources. Second, the storage of a large amount of hydrogen in a small and light vessel is difficult due to the low volumetric energy density of hydrogen; nevertheless, the main drawback remains in hydrogen production and storage [3, 4]. Among the different hydrogen storage methods, chemical hydrides arise as the major compounds to address these concerns. In particular, sodium borohydride ($NaBH_4$) is one of the most attractive chemical hydrides to storage and generate hydrogen, due to its high hydrogen content (10.8 wt%) as well as high energy density, combined with a good storage stability and nontoxicity [3, 5]. Through a simple hydrolysis reaction it is possible to produce pure molecular hydrogen adding a stoichiometric amount of water to sodium borohydride. However, the rate of hydrogen generation from self-hydrolysis of sodium borohydride is not satisfactory

[1](born May, 1960) U.S. Representative for Pennsylvania's 15th congressional district.

without the addition of a suitable catalyst [6]. Therefore, various metal catalysts have been developed. The present work focuses on a bimetallic nickel-ruthenium based catalyst, in the form of a finely divided powder to generate hydrogen by sodium borohydride hydrolysis.

In order to provide energy to portable applications, studies of sodium borohydride hydrolysis reaction in a small stainless steel reactor (≈ 9 cm^3) were carried out for the first time. This thesis studies the reactor design and material compounds to ensure better efficiency in hydrogen production. Nevertheless, further studies should be conducted, to deepen this innovative idea and ensure maximum profitability of the designed reactor.

1.2 Objectives

The purpose of the present work focuses on the synthesis of hydrogen from catalytic hydrolysis of sodium borohydride, maintaining high yielding rates at "moderate pressure" (up to 30 bar) and room temperature.

To achieve this goal, a portable mini-reactor with an ovoid optimized geometry was designed, to generate and storage H_2. The reactor material was chosen considering the following factors: 1) hydrogen diffusion effect; 2) hydrogen embrittlement effect; 3) material density – the reactor should be the lightest possible and 4) material costs. Then, experiments of alkali free hydrolysis of $NaBH_4$ were performed, in the presence of a reused Ni-Ru based catalyst, in order to assess the following parameters: 1) $H_2O/NaBH_4$ ratio; 2) catalyst/$NaBH_4$ ratio and 3) temperature. Since most of the studies in this area reports an H_2 production from aqueous alkaline solution of $NaBH_4$, the effect of the presence of sodium hydroxide (NaOH) was also evaluated.

It is expected that the obtained results of the present work thesis contribute to an efficient H_2 production regarding high energy density and hasten the acceptance of $NaBH_4$ as the elected H_2 carrier in PEMFC portable applications.

1.3 Overview

The thesis outline involves six main chapters.

Chapter 1, *Introduction*:

Introduces the research subject and presents the main objectives of this dissertation.

Chapter 2, *State of the art*:

This chapter contains background information about the potential of hydrogen as an energy carrier and sodium borohydride as an energy/hydrogen carrier. Reports a literature review of the most efficient catalysts used in sodium borohydride hydrolysis reaction, with special emphasis for the ruthenium based catalyst, and a broad introduction to polymer electrolyte membrane fuel cells.

Chapter 3, *Experimental techniques and apparatus*:

This chapter describes the experimental procedures, techniques and apparatus used in this work. It also details the theory behind the novel mini-reactor designed and offers a brief reference to the experimental approach.

Chapter 4, *Results and discussion*:

This chapter offers a profitable discussion about the importance of considering the reactor design effects on the performance of sodium borohydride hydrolysis reaction. For high density hydrogen generation, a set of experimental tests were performed with a stoichiometric amount of water in the presence of a nickel-ruthenium based catalyst, this latter reused about ≈47 times. Also characterize the catalyst by its activation energy, and referred a literature overview comparison.

Chapter 5, *Conclusions*:

Presents the main conclusions of the developed work and gives suggestions for further studies, which could contribute to this area of research.

Chapter 6, *References*:

Indicates the bibliographic references used in this dissertation.

2 State of the art

"If we had a hydrogen economy worldwide, every nation on earth could create its own energy source to support its economy, and the threat of war over diminishing resources would just evaporate." Dennis Weaver[2]

2.1 Hydrogen as an energy carrier

In recent years, the global energy system focused predominantly on the utilization of fossil fuels, coal, oil and natural gas, which comprises more than 85% of the primary world energy production. Owing to this, implementing effective policies and measures to mitigate global warming, improve air quality and reduce energy consumption arise as the major challenges for global climate and energy policy [7, 8].

The ideal future goes through a world of renewable and pollution free energy sources, to sustain every quotidian habit, from electrical power grids to personal vehicles. Hydrogen is likely to be part of this idealistic future, and possibly an important fraction. In fact, hydrogen is the most abundant and simple element of the Universe. It is colourless, odourless, tasteless and the smallest and lightest molecule in the world. Table 1 summarizes some of the properties of hydrogen [9, 10].

Since hydrogen is not naturally available as a ready-to-use substance, it cannot be considered an energy source. Nevertheless, it has high potential as an energy carrier, due to the high energy density of 142 MJ kg^{-1}, almost three times more than the average value of petroleum (47 MJ kg^{-1}). Additionally, hydrogen can be used directly in a PEMFC, which offers a higher efficiency (50-60%) than most combustion engines (<25%), turning hydrogen the ideal source of energy [11, 12]. The PEMFC allows the generation of electricity, yielding only water as a by-product. This type of fuel cell has been widely accepted in portable applications, since it operates at low temperatures and offers a high power density. However, PEMFC also entails certain disadvantages, namely the requirement of pure hydrogen [10]. A further explanation of PEMFC is provided forward, in chapter 2.3.

[2](born June, 1924 – die February, 2006) American actor.

Table 1| Molecular hydrogen properties [12].

Property	Value
Name / Symbol / Number	Hydrogen / H / 1
Atomic weight	1.008
Electrons / Protons / Neutrons	1 / 1 / 0
Colour / Odour	Colourless / Odourless
Toxicity	None, simple asphyxiant
Phase	Gas
Density	Gas: 0.089 g/L ; Liquid: 0.07 g cm^3
Ionization Energy	13.5989 eV
Liquid to gas expansion rate	1:848 (atmospheric conditions)
Melting and boiling point	-259.14 °C ; -252.87 °C
Lower heat value	118.8 MJ kg^{-1}
Adiabatic flame temperature	2107 °C
Flammability range in the air	4-75 %
Laminar flame velocity	3.06 m s^{-1}
Flash point	-253 °C
Auto ignition temperature	585 °C
Research octane number	>130

Hydrogen presents some features that turn it a unique energy carrier, namely the exceptional energy per mass content, safety features and reduced harmful emissions. On the other hand, hydrogen presents very low density in the gaseous state, turning the storage of a sufficient amount of hydrogen in a small and light vessel a significant challenge. In fact, hydrogen storage has proved to be the greatest obstacle to replace fossil fuels. Thus, a further research in this area is needed to turn viable a hydrogen economy based on renewable energies [4, 12]. So, what is the hydrogen economy?

The hydrogen economy is a system that uses hydrogen as a major carrier in the energy supply cycle. The term evokes a vision of a usage of energy in the future that is sustainable and environmentally friendly. That vision follows the historical trend toward using energy sources that produce less and less carbon as a by-product [9].

The majority of developed countries, such as U.S. of America and Japan, has already come up with strategies to transit to hydrogen economy and has already started their implementation. Recently, the U.S. Department of Energy (DOE) published *A*

National Vision of America's to Hydrogen Economy to 2030 and Beyond. This document summarizes the potential role for hydrogen systems in America's energy future, outlining the common vision of the hydrogen economy [7, 13].

To be a successful energy carrier, hydrogen must be economically competitive, and the individual technological components must be connected via an infrastructure that provides a safe and environmentally acceptable energy system throughout the whole production, distribution and end-use chain. Over the past decades, hydrogen has been used in different application fields (such as chemical processes, propellant for rockets, coolant in generators, etc.). Consequently, from historical perspective, hydrogen safety research is scattered. Moreover, only a small number of hydrogen and fuel cell systems and components required for the hydrogen economy are in operation today. Therefore, only limited data is available on the operational and safety aspects of these new technologies and research is required to understand hydrogen behavior as a fuel for portable applications [14].

2.2 Chemical hydrides as a hydrogen carrier

According to its abundance, hydrogen can be extracted from a variety of material and compounds or be produced using a wide range of methods, including some clean and "green" approaches. More importantly, hydrogen can be synthesized anywhere across the planet [12]. Among the different hydrogen storage methods, chemical and metal hydrides exhibit an impressive theoretical volumetric hydrogen storage density on a material basis and, therefore, they are established as the most promising hydrogen storage resources for portable applications. In particular, $NaBH_4$ and ammonia borane (NH_3BH_3) are pointed as the chosen hydrogen carriers, due to their high gravimetric hydrogen storage capacity (GHSC) and volumetric hydrogen storage capacity (VHSC), 10.8 wt% and 19.6 wt% for GHSC and 113 and 152 kg m^{-3} for VHSC, respectively. However, accordingly to Demirci *et al.* (2009) [15], hydrolysis of $NaBH_4$ seems to be more suitable for portable applications [15, 16].

2.2.1 The special case of sodium borohydride

Sodium borohydride was synthesized for the first time in 1942, by Prof. H. C. Brown (1912-2004), Nobel Laureate in Chemistry in 1972, and Prof H. I. Schlesinger, due to the military interest in its potential as a hydrogen generator. The 20 years that followed this landmark were characterized by an intense research. Nevertheless, the research about $NaBH_4$ as energy/hydrogen carrier stopped until late 1990s, when

$NaBH_4$ has drawn scientists' attention to itself again. The context of those "re-investigations" was critical from both energy and environmental points of view [15].

In 2009, the U.S. DOE revised the previous 2015 targets and added a new category, the "Ultimate Full Fleet" target. This category aimed to facilitate the introduction of hydrogen economy structures on the reaction system designs for fast hydrogen generation. The "Ultimate Full Fleet" set targets are 70 g_{H_2} L^{-1} and 7.5 wt% H_2. A reactor with an ovoid geometry could be the "key" to attain these targets [17, 18].

$NaBH_4$ reacts with water (H_2O) to generate molecular hydrogen according to the following equation, where ***x*** represents the hydration factor:

$$\mathrm{NaBH_4} + (2+x)\mathrm{H_2O} \rightarrow \mathrm{NaBO_2} \cdot x\mathrm{H_2O} + 4\mathrm{H_2} + \mathrm{heat} \qquad \text{(Eq.1)}$$

The hydrolysis of $NaBH_4$ is a spontaneous, exothermic reaction (-210 kJ mol^{-1}) that can be accelerated due to a well-chosen metal-based catalyst [3].

A critical issue in developing an efficient hydrogen generator from $NaBH_4$ is the amount of water needed in the reaction end. Ideal hydrolysis is attained for ***x***=0, where 2 mol of water are required to react with 1 mol of solid $NaBH_4$ to liberate 4 mol of hydrogen. However, in practice, excess of water is necessary for two reasons: 1) low solubility of $NaBH_4$ and $NaBO_2$ in water (55 g $NaBH_4$ per 100 g H_2O at 25 °C and 28 g $NaBO_2$ per 100 g H_2O at 25 °C) and 2) the fact that the stable form of the reaction by-product, $NaBO_2$, is its hydrated form ($NaBO_2 \cdot xH_2O$) and consequently, the water excess leads to a decrease of the hydrogen storage density [4, 19].

Figure 1 shows the U.S. DOE FreedomCar targets for automotive hydrogen storage systems up to 2015 [20]. Capacities above 9 wt% in 2015 are expected, which, according to the evolution of GHSC of the fuel [$NaBH_4$ + (2+***x***)H_2O] shown in Figure 2, can only be possible when ***x*** assumes values below 0.84. However, that is a mistake that is often made throughout the open literature. The GHSC is generally calculated on the basis of only $NaBH_4$ and water, while this must be done on the basis of the complete storage system, including reactors, tanks, valves and all the supplementary equipment.

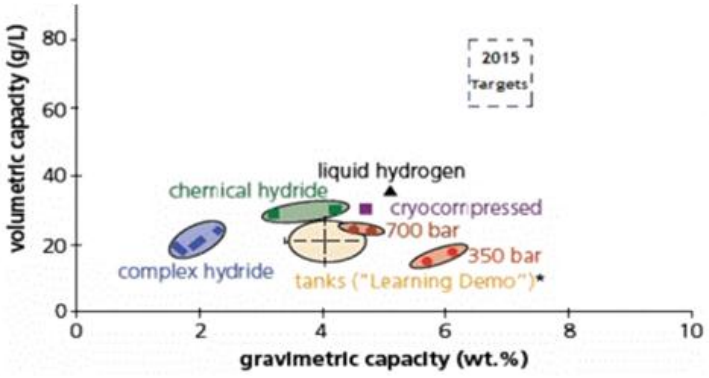

Figure 1| Volumetric and gravimetric capacities for several possible hydrogen storage technologies [20].

Thus, producing hydrogen with even higher GHSC to supply on-demand a PEMFC, i.e. exclude any excess of water (x=0), is one of the main objectives of the present study [3, 10, 21].

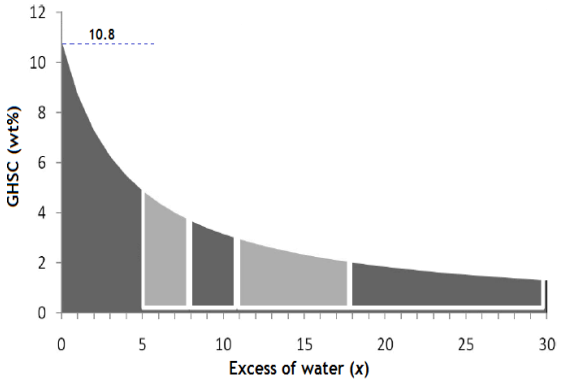

Figure 2| Evolution of the GHSC of the fuel [$NaBH_4$ + (2+x)H_2O] with excess of water [3].

2.2.2 Catalyst overview

At room temperature and without a catalyst, only a negligible amount of hydrogen is released during the hydrolysis of $NaBH_4$. By adding a suitable catalyst, the hydrogen generation rate is significantly enhanced [22, 23].

In 1953, Schlesinger *et al.* (1953) [24] studied the accelerating effects of acids and the transition metal compounds on $NaBH_4$ hydrolysis reaction. With this study, the authors concluded that an effective catalyst is the heart of the hydrolysis reaction of $NaBH_4$. Table 2 presents not only the results published by Schlesinger *et al.* (1953) [24] but also the results obtained by Liu *et al.* (2006) [25], which in 2006 use cobalt salts to study the catalyzed hydrolysis of sodium borohydride.

Table 2| Literature overview for catalyst salts.

Catalyst	Catalyst/Support (Amount [g], Loading [wt%])	HGR (L_{H2} min^{-1} g_{Cat}^{-1})	$NaBH_4$ Concentration (wt%)	Temperature (°C)	GHSC (wt%)	Ref.
$FeCl_2$	0.15 g	1.70	n/a	25	1.00	[24]
$CoCl_2$	0.15 g	3.70	n/a	25	1.00	[24]
$CoCl_2$	0.50 g	0.60	1.00	10	0.20	[25]
$CoCl_2$	0.50 g	11.40	1.00	20	6.80	[25]
$NiCl_2$	0.15 g	2.50	n/a	25	1.00	[24]
$CuCl_2$	0.15 g	1.20	n/a	25	1.00	[24]

As catalysts play such a role in hydrogen generation from $NaBH_4$ hydrolysis, numerous substances have been developed to increase this rate. These substances include noble transition metals, such as ruthenium (Ru), platinum (Pt), palladium (Pd), Pt-Ru and Pt-Pd alloys, and non-noble transition metals, such as cobalt (Co), nickel (Ni) borides, and others [26, 27].

Table 3 presents a literature overview for non-noble transition metals catalysts [25, 28–41]. Zhuang *et al.* (2013) [34] obtained the highest hydrogen generation rate ever reported (with a Co-Mo-B catalyst) to produce 6.43 wt% H_2 by sodium borohydride catalyzed hydrolysis. Therefore, the presence of molybdenum in the catalyst, and its influence, arises as a promising element of study in catalytic sodium borohydride hydrolysis.

A literature overview for noble transition metals catalysts [4, 16, 42–59], including the main results from this thesis, is presented in Table 4. The importance of ruthenium based catalyst appears to be relevant to achieve highest results (HGR and GHSC) in catalytic sodium borohydride hydrolysis. Moreover, the catalysts with ruthenium present a high reuse property, which is economically significant.

Is noteworthy that with exception of the present work, as well as Ferreira *et al.* (2010) [4] results were calculated at moderate pressure. The remaining results were obtained at atmospheric pressure.

Table 3| Literature overview for non-noble metal catalysts.

Catalyst	Catalyst/Support (Amount [g], Loading [wt%])	Reuse	E_A (kJ/mol)	HGR (L_{H2} min^{-1} g_{Cat}^{-1})	$NaBH_4$ Concentration (wt%)	Temperature (°C)	GHSC (wt%)	Ref.
Co-B	0.05 g	0	64.87	1.10	20.00	20	4.20	[28]
Co-B	0.05 g	0	64.87	2.80	20.00	30	4.20	[28]
Co-B	0.10 g	0	n/a	3.00	2.00	15	0.40	[29]
Co_3-B	0.03 g	n/a	n/a	6.00	5.00	60	1.10	[30]
Co-B-Ni	n/a	0	33.00	11.00	20.00	30	4.20	[31]
Co-B-Ni	n/a	0	44.47	1.60	5.00	25	1.10	[32]
Co-W-B-Ni	10.00 g	6	29.00	15.00	20.00	30	4.20	[33]
Co-Mo-B	0.02 g	0	n/a	113.10	31.25	25	6.43	[34]
Ni-Co-B	0.10 g	0	62.00	2.60	2.70	28	0.70	[35]
Ni_3-B	0.05 g	0	n/a	1.30	10.00	60	2.10	[30]
Ni_x-B	0.10 g	0	38.00	0.30	1.50	20	0.30	[36]
Ni-B-SiO_2	0.65 g	3	60.70	1.90	0.11	25	0.10	[37]
Co powder	0.50 g	0	41.90	0.10	1.00	20	0.20	[25]
Raney Co	0.50 g	0	53.70	0.30	1.00	20	0.20	[25]
Co-PPX-Cl	n/a	0	n/a	4.30	2.50	25	0.50	[38]
Filamentary Ni-Co	1.00 g , 20 wt%	200	n/a	0.10	10.00	30	3.30	[39]
Ni nanoclusters	0.80 g	n/a	54.00	1.70	0.56	25	0.10	[40]
Raney Ni	0.50 g	0	50.70	0.20	1.00	20	0.20	[25]
Raney $Ni_{50}Co_{50}$	0.50 g	0	52.50	0.70	1.00	20	0.20	[25]
Co-γAl_2O_3	0.05 g , 9 wt%	n/a	32.63	0.22	5.00	30	3.20	[41]

Table 4| Literature overview for noble metal catalyst.

Catalyst	Catalyst/Support (Amount [g], Loading [wt%])	Reuse	E_A (kJ/mol)	HGR (L_{H2} min^{-1} g_{Cat}^{-1})	$NaBH_4$ Concentration (wt%)	Temperature (°C)	GHSC (wt%)	Ref.
Pt-C	0.25 g , 1 wt%	0	n/a	2.90	2.00	20	0.40	[42]
Pt-C	0.25 g , 2 wt%	0	n/a	0.17	5.00	30	1.10	[43]
Pt-C	0.10 g , 20 wt%	0	n/a	23.09	10.00	20	2.10	[44]
Pt-$LiCoO_2$	0.26 g , 1.5 wt%	n/a	n/a	3.10	20.00	22	4.20	[45]
Pt-$LiCoO_2$	240.00 g , 1.5 wt%	0	n/a	0.50	25.00	110	2.00	[46]
Pt-$LiCoO_2$	0.24 g , 10 wt%	n/a	n/a	0.63	5.00	25	2.10	[47]
Pt-Ru-$LiCoO_2$	0.13 g , 10 wt%	n/a	n/a	2.40	5.00	25	2.10	[47]
Pt-Ru-$LiCoO_2$	0.08 g , 10 wt%	0	n/a	3.60	5.00	25	1.10	[48]
Pt-γAl_2O_3	0.25 g , 2 wt%	0	n/a	0.10	5.00	30	0.80	[43]
Pt-TiO_2	0.25 g , 1 wt%	0	n/a	0.04	2.00	20	0.40	[49]
Pt-Ag-TiO_2	0.25 g , 1 wt%	0	n/a	0.03	2.00	20	0.40	[49]
Pt-Ru-Co_3O_4	0.08 g , 10 wt%	0	n/a	12.00	5.00	25	1.10	[48]
Rh-C	1 wt%	0	n/a	0.65	0.46	40	0.10	[50]
Rh-$LiCoO_2$	0.01 g , 1 wt%	n/a	n/a	7.32	4.50	40	0.50	[51]
Rh-γAl_2O_3	1 wt%	0	n/a	0.27	0.46	40	0.10	[50]
Rh-TiO_2	1 wt%	0	n/a	1.82	0.46	40	0.10	[50]
Pd-C	1 wt%	0	n/a	0.05	0.46	40	0.10	[50]
Pd-TiO_2	1 wt%	0	n/a	0.12	0.46	40	0.10	[50]
Ru	0.50 g , 2 wt%	n/a	n/a	2.00	20.00	23	4.30	[52]

Ru	0.50 g , 2 wt%	n/a	n/a	2.10	25.00	23	5.20	[52]
Ru	0.25 g	n/a	n/a	0.72	20.00	22	3.80	[53]
Ru-C	0.20 g , 3 wt%	0	83.50	0.80	1.00	25	0.20	[54]
Ru-$LiCoO_2$	0.13 g , 10 wt%	n/a	n/a	1.12	5.00	25	2.10	[47]
Ru-γAl2O3	0.50 g , 2 wt%	0	54.90	4.80	12.00	30	2.50	[55]
Ru-TiO_2	0.25 g , 1 wt%	0	n/a	0.16	2.00	20	0.40	[49]
Ru-Cu-TiO_2	0.25 g , 1 wt%	0	n/a	0.03	2.00	20	0.40	[49]
Ru-Pd-TiO_2	0.25 g , 1 wt%	0	n/a	0.06	2.00	20	0.40	[49]
Ru-Pt-TiO_2	0.25 g , 1 wt%	5	n/a	0.15	2.00	20	0.40	[49]
Ru-Ag-TiO_2	0.25 g , 1 wt%	0	n/a	0.04	2.00	20	0.40	[49]
Ru-$ZrO_2^-SO_4^{2-}$	0.25 g , 1 wt%	0	n/a	10.50	2.00	20	0.40	[42]
$Ru_{60}Co_{40}$	2.50×10^{-3} g	n/a	n/a	17.50	10.00	25	2.10	[56]
$Ru_{80}Fe_{20}$	2.50×10^{-3} g	n/a	n/a	18.30	10.00	25	2.10	[56]
$Ru_{60}Co_{20}Fe_{20}$	2.50×10^{-3} g	n/a	n/a	26.80	10.00	25	2.10	[56]
Ru-IRA 400	0.25 g , 5 wt%	n/a	56.00	0.20	20.00	25	4.20	[57]
Ru-IR120	0.20 g , 1 wt %	0	49.72	0.13	5.00	25	0.14	[58]
Ni-Ru	0.24 g , 1.42 wt%	320	n/a	87.40	45.20	25	8.10	[16]
Ni-Ru	0.48 g , 1.42 wt%	150	n/a	24.20	10.00	25	6.30	[4]
Ni-Ru	0.48 g , 1.42 wt%	266	n/a	33.00	30.00	25	6.10	[59]
Ni-Ru	0.02 g	47	75.12	0.05	46.00	22	7.87	This work
Ni-Ru	0.02 g	47	75.12	7.90	46.00	55	0.76	This work
Ni-Ru	0.02 g	47	75.12	57.12	46.00	55	5.88	This work
Ni-Ru	0.02 g	48	75.12	1.02	10.00	22	2.29	This work

2.3 Polymer Electrolyte Membrane Fuel Cell

As already stated, hydrogen cannot be considered an energy source, since it is an intermediary form of energy. In fact, the energy vector hydrogen can be compared to electricity – it can be generated from a variety of energy sources and be delivered to the end users, being converted efficiently and cleanly to useful energy. The means for hydrogen conversion into energy have been developed in the last years. Hydrogen combusts, so it can be used as a fuel in a turbine engine and also in an internal combustion engine, either alone or mixed with other fuel. However, the main research and development have been focused on fuel cells [60].

The fuel cell is a device that uses electrochemical means to convert the chemical energy of fuel into electricity and heat, and produces only a harmless by-product, namely water. Typically, fuel cells reactants are hydrogen and oxygen; however, none of them need to be in its pure form. Therefore, fuel cells can use a variety of primary fuel that contains hydrogen, such as natural gas and methanol, and, with respect to oxygen, it can be used from ambient air [60, 61].

Fuel cells systems have the potential to be significantly more efficient than a coal fired power station or an internal combustion engine. A fuel cell can achieve 50-60% efficiency. Moreover, it has no moving parts and presents a lower maintenance cost and an operating life longer than an internal combustion engine. Besides these advantages, fuel cells decrease pollution and are less noisy than the others combustion engines [61].

The first demonstration of the fuel cell principle is awarded to Sir William Grove, who in 1839 produced electricity from hydrogen and oxygen by reversing water electrolysis. Figure 3 shows a smaller four cell's version of Grove's experimental set-up. Briefly, separate platinum electrodes are halfway immersed in a dilute solution of sulphuric acid and water, and the other half is sealed in inverted hydrogen and oxygen gas containers, generating a small current. The electrolysis is reversed, i.e. the hydrogen and oxygen recombine and an electric current is being produced [62, 63].

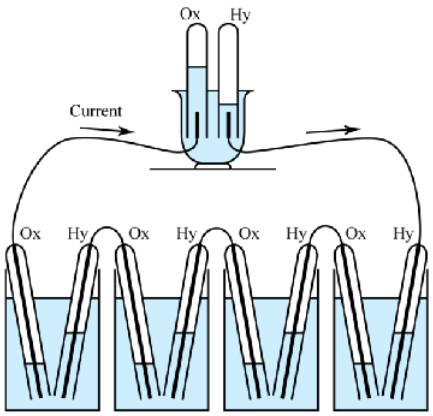

Figure 3| "The gaseous voltaic battery", the first fuel cell by William Grove [63].

William Grove invention, known as the "gaseous voltaic battery", remained as a scientific curiosity for almost a century. Only in the twentieth century, during World War II, the British scientist Francis Bacon started working on practical fuel cells, developing a 6 kW fuel cell stack in 1959. However, the first practical fuel cells applications were used by NASA in the U.S. Space Program, in the early 1960s [60, 62].

Due to the NASA Program success, the fuel cells development increased and, currently, there are six main types of fuel cells of commercial importance for energy production, either in stationary or transportation applications: Alkaline Fuel Cell (AFC), Phosphoric Acid Fuel Cell (PAFC), Molten Carbonate Fuel Cell (MCFC), Solid Oxide Fuel Cell (SOFC), Polymer Electrolyte Membrane Fuel Cell (PEMFC) and Direct Methanol Fuel Cell (DMFC) [60, 61].

Table 5 resumes the characteristics of these fuel cells, as well as their advantages and disadvantages.

Table 5| Types of fuel cells [61].

Fuel cell	Temperature (°C)	Efficiency (%)	Application	Advantages	Disadvantages
Alkaline fuel cell (AFC)	50-90	50-70	Space application	High efficiency	Intolerant to CO_2 in impure H_2 and air, corrosion, expensive
Phosphoric acid fuel cell (PAFC)	175-220	40-45	Stand-alone & combined heat & power	Tolerant to impure H_2, commercial	Low-power density, corrosion & sulfur poisoning
Molton carbonate fuel cell (MCFC)	600-650	50-60	Central, stand-alone & combined heat & power	High efficiency, near commercial	Electrolyte instability, corrosion & sulfur poisoning
Solid oxide fuel cell (SOFC)	800-1000	50-60	Central, stand-alone & combined heat & power	High efficiency & direct fossil fuel	High temperature, thermal stress failure, coking & sulfur poisoning
Polymer electrolyte membrane fuel cell (PEMFC)	60-100	40-50	Vehicle & portable	High power density, low temperature	Intolerant to CO in impure H_2 and expensive
Direct methanol fuel cell (DMFC)	50-120	25-40	Vehicle & small portable	No reforming, high power density & low temperature	Low efficiency, methanol crossover & poisonous by product

According to Table 5, the PEMFC is the leading contender for use in vehicles and in portable applications. This device is lightweight, operates at low temperature, has a quick start-up and uses a solid membrane, which are advantages for mass consumer operation. The membrane electrode assembly (MEA) is the key factor of the cell. It consists in a polymer electrolyte membrane with a catalyst layer in each side, and it is located between a pair of current collector plates with machined flow fields for distributing fuel and oxidant to anode and cathode, respectively [61, 62, 64].

Hydrogen and oxygen are supplied to the anode and the cathode, respectively. The hydrogen splits into electrons and protons (H^+) due to the catalyst present in the anode. The liberated electrons provide the electrical output, while protons pass through the electrolyte to recombine with oxygen, as well as with electrons on the cathode side to produce water. A brief scheme of the process is represented in Figure 4 [60, 62, 65].

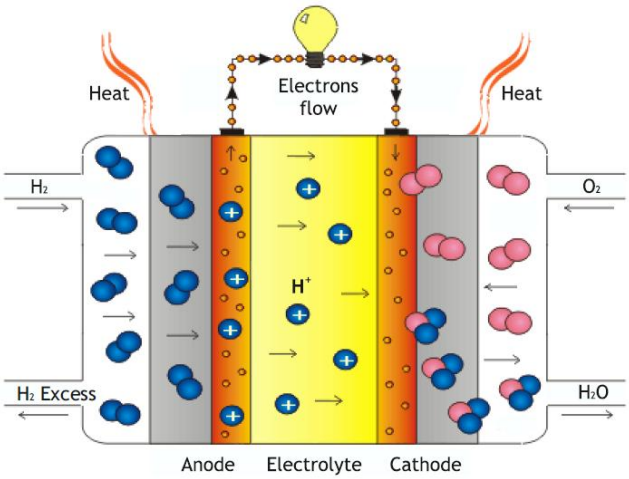

Figure 4| Schematic representation of a PEMFC (adapted from [65]).

The combustion of hydrogen into water is split into two electrochemical reactions occurring at the anode and the cathode, which are termed as the two half-cell reactions:

Anode: $H_2 \rightarrow 2H^+ + 2e^-$ (Eq.2)

Cathode: $½O_2 + 2H^+ + 2e^- \rightarrow H_2O$ (Eq.3)

Overall reaction: $H_2 + ½O_2 \rightarrow H_2O$ (Eq.4)

The role of the electrolyte is crucial, since it insulates the two half-cell reactions electrically in a strict sense while allowing the ionic passage of protons produced at the anode to the cathode side.

The best known and established electrolyte material is the copolymer of tetrafluoroethylene and perfluoro[2-(fluorosulfonylethoxypropylviny]) ether, namely Nafion®, which was created by the DuPont Company. The catalyst layers are typically composed by platinum (or platinum-ruthenium) particles loaded into a carbon support [10, 60, 62].

3 Experimental Techniques and apparatus

"As we explore ways to bring price relief and bolster our country's energy independence, one significant energy source has emerged as a potential solution, hydrogen fuel cells." Dan Lipinski[3]

This chapter describes the experimental setup and procedure applied in the kinetic studies of the catalytic hydrolysis of sodium borohydride, as well as the materials used. It also describes all the factors that took impact on the novel mini-reactor specifications and design choices.

3.1 Materials

3.1.1 Sodium Borohydride

Anhydrous sodium borohydride powder (96% purity) was provided by Panreac (123314.1608) and stored in a desiccator until use.

In alkali free hydrolysis experiments, the sodium borohydride was used in the solid state. However, to study sodium hydroxide influence, $NaBH_4$ stabilized solutions were prepared by the addition of small quantities of sodium hydroxide pellets (98% purity) as hydrolysis inhibitors. The NaOH used was supplied by EKA (No.: 1310.73.2)

3.1.2 Nickel based bimetallic catalyst

All the experiments were carried out on the presence of a nickel-ruthenium based catalyst, with nanometric particle size, synthesized at LNEG – Laboratório Nacional de Energia e Geologia, Fuel Cells and Hydrogen Unit, Lisbon – Portugal, in November 2012.

Until the experiments reported in this work were performed, the catalyst was already used 46 times. Moreover, this catalyst was chemically similar to the one used by Ferreira MJF *et al.*[4, 16, 18, 19, 59] in all the experiments. Considering this, the catalyst preparation for this thesis was the same reported by Ferreira MJF *et al.* [18]. Briefly, the nickel based bimetallic unsupported catalyst was in the form of a finely divided black powder. This compound was prepared from the impregnation

[3](born July, 1966) U.S. Representative for Illinois's 3rd congressional district.

of a mixture of ruthenium and nickel salts (Riedel-de Haën) in deionised water, by chemical reaction with 10 wt% stabilised borohydride solution (Rohm and Haas), as the reducing environment. When the reduction was complete, the catalyst was appropriately decanted, washed, filtered, dried and heat-treated at 110 ºC.

Figure 5 shows a scanning electron microscope (SEM) image and the respective energy-dispersive X-ray (EDX) spectrum of the *fresh* Ni-Ru based catalyst. The SEM micrograph (Fig.5A) shows a homogenous ruthenium distribution and the EDX spectrum showing a very small amount of ruthenium as part of the catalyst composition (the amount of ruthenium was not always detectable by EDX, however a concentration of 0.74 At% was obtained by X-ray photoelectron spectroscopy (XPS)). It is important to highlight that the present catalyst was optimized to work at 45ºC, and was already used 46 times in several studied schemes of $NaBH_4$ hydrolysis for H_2 generation. A detailed study of the oxidation state of the catalyst components and of its aging is published elsewhere [59].

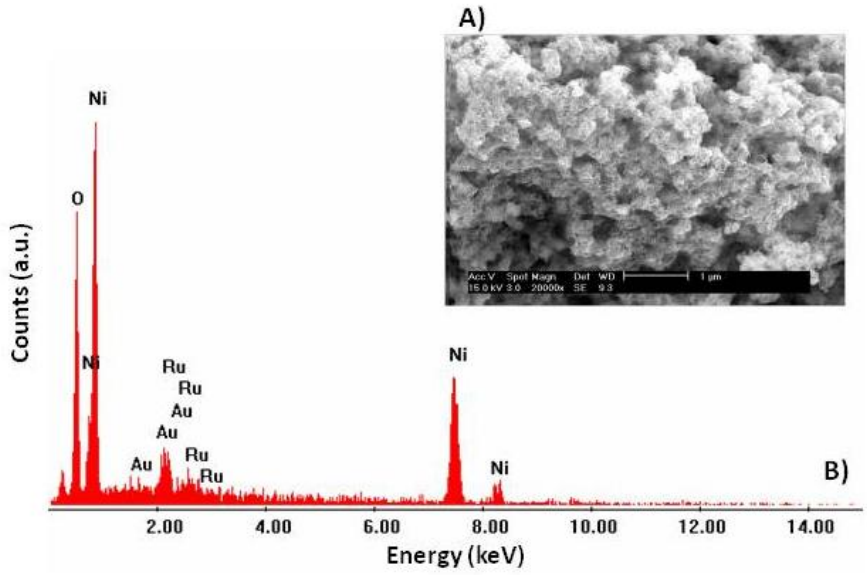

Figure 5| A) Photo scanning electron microscope view of the synthesized catalyst powder. B) Associated elemental EDAX. [10]

3.2 Egg-shaped mini reactor

The hydrogen economy for portable consumer products requires a simple and safe technology for its storage and on-demand production. Besides that, it is noteworthy that all the hydrogen storage capacities reported in chapter 2.2.2 are calculated on a reactants only basis, i.e. they do not take on account the mass of the reactor,

valves, etc., which must be considered when comparing the storage capacities to the DOE targets [10, 53].

For example, Kojima *et al*. (2004) [46] reported that a 25 wt% $NaBH_4$ solution on a reactant only basis would produce 5.3 wt% H_2. Nevertheless, when the mass of the entire system is also taking in account, the hydrogen storage capacity reduces to 2.0 wt%. This decrease is mostly due to the reactor tanks, which represents the difficulty associated with the reactor design in meeting the DOE storage targets on a weight of system basis.

Although related works have reported the utilization of cylindrical reactors, almost with flat bottom, Ferreira *et al*. (2010) [4] remarked that a conical bottom reactor increases both the hydrogen yield and generation rates, and decreases the induction time. A plausible explanation for these observations is that a conical bottom shape enhances the contact between $NaBH_4$, catalyst and the injected water leading to a decrease of mass transfer resistances.

Later, the same authors [18] observed that, at the end of the experiments, the top of the reactor accumulated condensed water derived from its evaporation. This fact probably occurred during the first period of the hydrolysis reaction, characterized by an increase of temperature, where faster H_2 rates were detected.

This physical phenomenon is probably one of the responsible factors for the non-complete hydrogen generation reaction, since it interdicts the availability of the water in the reaction medium, precluding the completeness of the reaction.

Those observations were the basis for the development of this master thesis, which is based on the design of a mini-reactor with a new geometry. Thus, the present work focuses on the design of an innovator portable reactor with reduced weight and size, and an egg-shaped geometry.

3.2.1 Reactor material

The first step on the ovoid shape reactor optimization was the choice of a building material that enhanced hydrogen compatibility, safety and reliability. There are several compounds to build an efficient lightweight reactor capable to store hydrogen, such as titanium, carbon nanotubes and polyether ether ketone (PEEK) polymer. Nevertheless, these materials entail high costs, which have facilitated the material choice used in the current project. Therefore, the selected material to build the egg-shaped reactor was AISI 316L stainless steel.

3.2.2 Reactor dimensions

For the design of the egg-shaped reactor, the study of its dimensions was a key process, since the main goal of its construction relied on a portable device. Therefore, the final volume of the reactor was optimized to ≈9 cm^3, the approximated size of a small chicken egg. Moreover, the stipulated internal diameter was ≈2 cm.

According to the total volume of the ovoid reactor, its thickness was calculated considering three parameters: 1) stresses and deformations of the reactor; 2) hydrogen diffusion effect and 3) hydrogen embrittlement effect.

These parameters are explained in the following sections.

3.2.2.1 Stresses and deformations in egg-shaped reactor: Shell theory

The stresses and deformations of an egg-shaped reactor are estimated according to the Shell Theory. This theory bases on the following hypothesis:

- the thickness of the membrane is reduced when compared to the dimensions of the reactor, turning the bottom and top spherical closures constant;
- the stresses only act at the shell middle surface;
- the applied loading components per unit area of the shell surface present a normal and tangent direction to the shell middle surface;
- the radial stress is negligible when compared to the remaining stress factors;
- the membrane stress resultants (N_Φ and N_θ) are uniformly distributed along the shell thickness, as schematized in Figure 6 [66, 67].

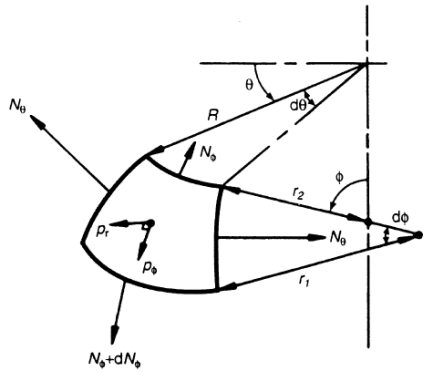

Figure 6| Element of an axisymmetrically loaded shell of revolution [67].

The ovoid reactor consists on spherical top and bottom closures of radius *r* and half-angle of opening Φ_0, that are connected by an ogival middle portion of meridional radius of curvature R_c, as schematized in Figure 7.

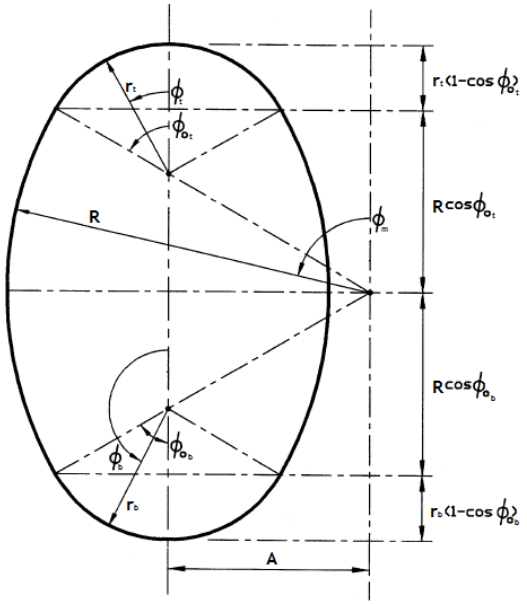

Figure 7| Geometric parameters of the shell of revolution comprising the egg-shaped reactor (adapted from [67]).

To determine the thickness of the reactor, the N_Φ and N_θ were calculated for the top, middle and bottom of the reactor, based on the following equations:

Top:

$$N_{\phi_t} = \frac{\gamma r_t^2}{6}\left(\frac{1-\cos\phi_t}{1+\cos\phi_t}\right)(1+2\cos\phi_t) \quad \text{(Eq.5)}$$

$$N_{\theta_t} = \frac{\gamma r_t^2}{6}\left(\frac{1-\cos\phi_t}{1+\cos\phi_t}\right)(5+4\cos\phi_t) \quad \text{(Eq.6)}$$

Middle:

$$N_{\phi_m} = \frac{1}{R_c\sin^2\phi_m - A\sin\phi_m}\left[\gamma A^2\left[A\frac{\cos^3\phi_m}{3} - \left(r_t + (R_c - r_t)\cos\phi_{0_t}\right)\frac{\cos^2\phi_m}{2}\right] - \gamma R_c A\left[\left(r_t + (R_c - r_t)\cos\phi_{0_t}\right)\sin\phi_m - R_c\left(\frac{\phi_m}{2} + \frac{\sin 2\phi_m}{4}\right)\right] + c_1\right] \quad \text{(Eq.7)}$$

$$N_{\theta_m} = \left(\frac{R\sin\phi_m - A}{\sin\phi_m}\right)\left[\gamma\left(r_t + (R_c - r_t)\cos\phi_{0_t} - R_c\cos\phi_m\right) - \frac{N_{\phi_m}}{R_c}\right] \quad \text{(Eq.8)}$$

The constant of integration c_1 is obtained from the condition that $N_{\Phi m}$ in the upper spherical shell and in the ogival shell must have the same values at the connection of these two regions (Φ_t=Φ_{0t}):

$$c_1 = \frac{\gamma r_t^2}{6}\left(\frac{1-\cos\phi_{0_t}}{1+\cos\phi_{0_t}}\right)\left(1+2\cos\phi_{0_t}\right)\left(R_c\sin^2\phi_{0_t} - A\sin\phi_{0_t}\right) - \gamma R_c^2\left[R_c\frac{\cos^3\phi_{0_t}}{3} - \left(r_t + (R_c - r_t)\cos\phi_{0_t}\right)\frac{\cos^2\phi_{0_t}}{2}\right] + \gamma R_c A\left[\left(r_t + (R_c - r_t)\cos\phi_{0_t}\right)\sin\phi_{0_t} - R_c\left(\frac{\phi_{0_t}}{2} + \frac{\sin 2\phi_{0_t}}{4}\right)\right] \quad \text{(Eq.9)}$$

Bottom:

$$N_\phi = \frac{1}{r_b\sin^2\phi_b}\left[-\gamma r_b^2\left(2(R_c - r_b)\cos\phi_{0_b} + r_b\right)\frac{\cos^2\phi_b}{2} + \gamma r_b^3\frac{\cos^3\phi_b}{3} + c_2\right] \quad \text{(Eq.10)}$$

$$N_\theta = \gamma r_b\left[2(R_c - r_b)\cos\phi_{0_b} + r_b(1-\cos\phi_b)\right] - N_{\phi_b} \quad \text{(Eq.11)}$$

Applying the condition that N_Φ in the ogival shell and in the lower spherical shell must have the same values at the connection of these two regions (Φ_b=Φ_{0b}):

$$c_2 = \gamma r_b^2\left[(R_c - r_b)\cos^3\phi_{0_b} + r_b\frac{\cos^2\phi_{0_b}}{2} + r_b\frac{\cos^3\phi_{0_b}}{3}\right] - \gamma R_c^2\left[\left(r_b + (R_c - r_b)\cos\phi_{0_b}\right)\frac{\cos^2\phi_{0_b}}{2} + R_c\frac{\cos^3\phi_{0_b}}{3}\right] - \gamma R_c A\left[\left(r_b + (R_c - r_b)\cos\phi_{0_b}\right)\sin\phi_{0_b} - R_c\left(\frac{\pi-\phi_{0_b}}{2} - \frac{\sin 2\phi_{0_b}}{4}\right)\right] + c_1 \quad \text{(Eq.12)}$$

In equations 5 to 12, γ represents the specific weight and Φ the angular coordinate (represented in Figure 7). The indices t, m and b correspond to top, middle and bottom, respectively.

To obtain the thickness of the reactor, h, the von Mises's yield criterion is applied to each of the three divisions of the egg-shaped reactor. This criterion states that:

$$\sigma_v^2 = \sigma_y^2 \quad \text{(Eq.13)}$$

Where σ_y is the yield strength of the material and the von Mises stress (σ_v^2) is calculated by the following equation:

$$\sigma_v^2 = \frac{N_\theta^2 - N_\theta N_\phi + N_\phi^2}{h} \quad \text{(Eq.14)}$$

Combining the both equations, the thickness of the reactor is easily calculated:

$$h^2 = \frac{N_\theta^2 - N_\theta N_\phi + N_\phi^2}{\phi_y^2} \quad \text{(Eq.15)}$$

All of the referred steps are thoroughly explained in Appendix A. Considering the Shell Theory [68], it can be concluded that the reactor needs to have a minimum thickness of 1.80 mm.

3.2.2.2 Hydrogen diffusion effect

Hydrogen is a small molecule with low molecular weight and low viscosity that easily diffuses through intact materials. The diffusion of hydrogen in metals and alloys is subject of numerous investigations, due to the important role of hydrogen-material interactions in a variety of fields, such as metallurgy, energy conversion and storage. Moreover, hydrogen escape from metal causes its crack and degradation [69, 70].

Owczarek *et al*. (2000) [71] have determined the hydrogen diffusivity in stainless steel samples presenting a thickness of 0.148 mm and 1 mm. The authors report that hydrogen escaped completely from samples with 0.148 mm and 1 mm thickness, after 280h and 6 weeks, respectively.

Taking in account the referred study and the fact that the generated hydrogen in this work will be inside the reactor in a period of time less than 6 weeks, it can be concluded that the reactor wall needs to have a minimum thickness of 1 mm, to prevent hydrogen losses by diffusion effects.

3.2.2.3 Hydrogen embrittlement effect

In 1875, W.H. Johnson observed for the first time a deleterious effect on the mechanical properties of iron caused by hydrogen. This phenomenon was called “hydrogen embrittlement”. Since that time, metals with outstanding combinations of high tensile strength and high fracture toughness have been developed with success. In particular, austenitic stainless steels are less susceptible to hydrogen cracking, due to their low diffusivity and high solubility of hydrogen in face centered cubic structures [72, 73].

Herms *et al*. (1999) [74] studied the deleterious effect on the mechanical properties of annealed AISI 316L stainless steel in wires with 1.5 mm diameter, in slow strain rate tests. Moreover, they also applied a precharging, with cathodically produced

hydrogen, of 24 hours duration to increase the severity of the tests. After 80 hours duration, the wires presented a strain to fracture of 20% and a crack depth of 0.14 mm.

Therefore, according to the results obtained by Herms *et al.* (1999) [74], it can be concluded that a thickness of at least 1.5 mm is enough to prevent the hydrogen embrittlement effect in the reactor.

Overall, based on all of the referred effects, the optimal thickness of the reactor was established to be 5 mm.

3.2.3 The final product

Based on all sections discussed in Chapter 3.2, the egg-shaped mini-reactor was built using the software program SolidWorks. Figure 8 schematizes the different 3D views of the projected reactor, where it can be seen a central ring with a larger thickness (≈12 mm). The presence of this ring is due to the necessity of inset measuring devices to control pressure and temperature inside the reactor.

Figure 8| Egg-shaped mini-reactor 3D views.

After the 3D draw was successfully completed, the reactor was built in Azemoldes Molding Technologies enterprise. A blueprint of the reactor is attached in Appendix B.

3.3 Analytical approach

3.3.1 Experimental setup

The experimental setup for the developed work, represented in Figure 9, comprised the egg-shaped reactor (Figure 10), previously discussed, a data acquisition system and a demonstration prototype with a PEMFC.

The data acquisition system consisted in two thermocouples, one pressure transducer and the Labview software. The thermocouples – one inside and another outside the reactor - allowed the following of temperature variation along the experiments. The inside thermocouple was used to monitor the increase of temperature in the core of the catalyzed exothermic hydrolysis reaction. On the other hand, the external thermocouple ensured the thermal isolation of the reactor, achieved by the internal mirroring and geometry of the device. The pressure transducer applied inside the reactor and calibrated from 0-40 bar, measured the gas pressure inside the ovoid reaction chamber, until attaining a constant pressure. This measurement was crucial, since the pressure inside the reactor is related with the hydrogen generation rate. This rate, as well as the thermocouple data, was recorded with Labview software.

The hydrogen synthesized in the different experiments was conducted to a PEMFC single cell placed inside of a didactic demonstration prototype, a mobile platform with a bus-like shape, designated “MicroBoro Bus”. Whenever hydrogen was being generated and fed to the PEM fuel cell, the wheels of “MicroBoro Bus”, which were connected to a small electric motor, swirled.

Figure 9 also shows the heating plate used to perform the controlled temperature studies, typically in the range of 45-60°C.

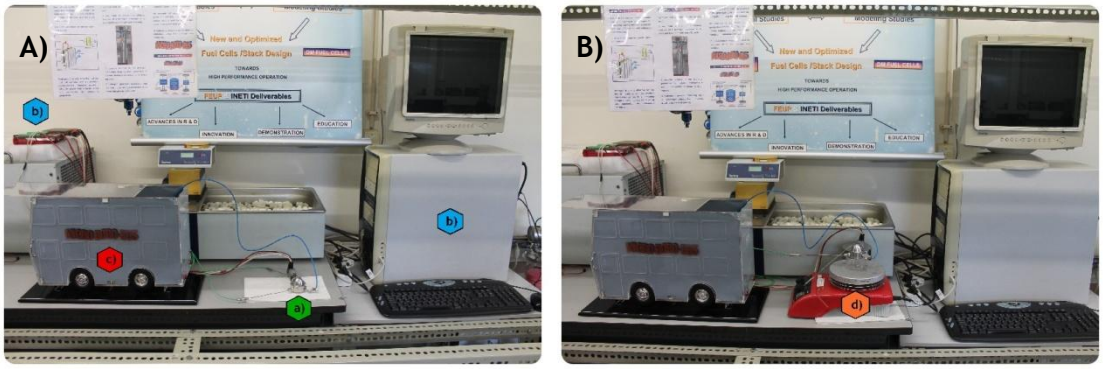

Figure 9| A) Experimental setup used for alkali free hydrolysis studies. B) Experimental setup of alkali hydrolysis tests.

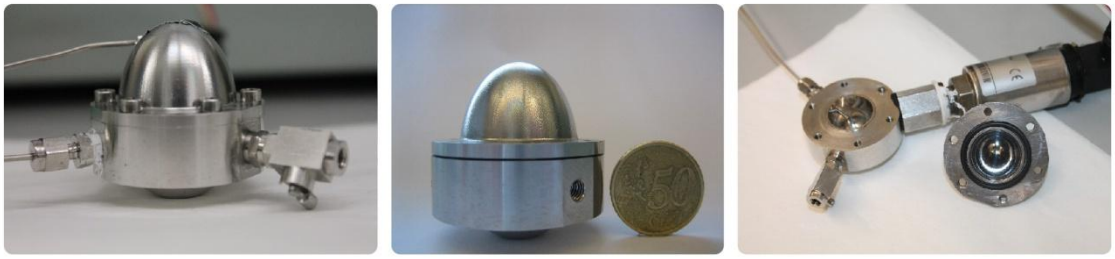

Figure 10| Egg-shaped mini-reactor perspectives.

3.3.2 Experimental procedure

To study the hydrogen production and storage, two different catalyzed sodium borohydride reactions schemes were performed: alkali-free hydrolysis and stabilized hydrolysis in the presence of an inhibitor.

The first type of reaction aimed to assess: 1) $NaBH_4$ amount; 2) water amount (***x***); 3) catalyst/$NaBH_4$ ratio and 4) temperature influence. The suitable $NaBH_4$ amount was determined through a preliminary study. This study presented an experimental procedure similar to the one used in all alkali-free hydrolysis reactions. Briefly, the required catalyst and $NaBH_4$ amount was added to the bottom of the reactor and mixed. The reactor was then sealed and the appropriate amount of water was immediately injected through a micro-syringe with a long needle, to guarantee that the water was precisely added close to the catalyst/$NaBH_4$ mixture.

The second type of reaction (alkali hydrolysis) aimed to evaluate the NaOH influence in hydrogen generation, a known inhibitor of this reaction. Foremost, two $NaBH_4$ stabilized solutions were equally prepared, with 1% and 7% of NaOH. To prepare these solutions, a specific amount of $NaBH_4$ was added to a certain volume of aqueous solution of NaOH. Then, the catalyst was added to the bottom of the reactor and it was properly sealed. Finally, the appropriate volume of $NaBH_4$ stabilized solution was injected using a mycro-syringe.

All of the reactions, with the exception of the temperature influence studies, were performed at uncontrolled room temperature. In the end of each reaction, the catalyst was recovered for reutilization. For that, it was washed four times with distilled water; then, it was separated from water by gravitational sedimentation and dried in an oven at 80 ºC during one hour.

4 Results and discussion

"Hydrogen is the ultimate fuel. It is clean, efficient, and yields more energy per unit of weight than any other existing fuel. Because hydrogen is a major component of water and of hydrocarbons, it is in abundant supply." Stanford R. Ovshinsky[4]

A detailed analysis of the obtained results, as well as the different studies performed in the reactor, will be described in this chapter. The presentation of the results and its discussion will be divided into two main groups – the alkali-free hydrolysis and alkali hydrolysis. The first one comprises the preliminary study and the effect of: 1) molar ratio $H_2O/NaBH_4$; 2) mass ratio catalyst/$NaBH_4$ and 3) temperature. The second group of reactions aims to study the effect of the NaOH inhibitor described in literature over hydrogen generation.

It is noteworthy that the parameters of yield (η), hydrogen generation rate (HGR), gravimetric (GHSC) and volumetric (VHSC) hydrogen storage capacities were equally calculated among all the experiments, by the following equations:

$$\eta\ (\%) = \frac{P_{Gas_{Exp.}}}{P_{Gas_{Theo.}}} \times 100 \qquad \text{(Eq.16)}$$

$$GHSC\ (\text{wt}\%) = \frac{m_{H_{2Exp.}}}{m_{NaBH_4}+m_{Cat.}+m_{H_2O}} \times 100 \quad \text{, for alkali-free hydrolysis} \qquad \text{(Eq.17)}$$

$$GHSC\ (\text{wt}\%) = \frac{m_{H_{2Exp.}}}{m_{Cat.}+m_{Sol.}} \times 100 \quad \text{, for alkali hydrolysis} \qquad \text{(Eq.18)}$$

Obs.: Although the reference in section 3.2 that GHSC should be measured in a material only basis, in the present work this parameter was calculated based in a reactant only basis, to facilitate the comparison with literature.

$$VHSC\ (\text{kg m}^{-3}) = \frac{m_{H_{2Exp.}}}{V_{NaBH_4}+V_{H_2O}+V_{Cat.}} \times 1000 \quad \text{, for alkali-free hydrolysis} \qquad \text{(Eq.19)}$$

$$VHSC\ (\text{kg m}^{-3}) = \frac{m_{H_{2Exp.}}}{V_{Cat.}+V_{Sol.}} \times 1000 \quad \text{, for alkali hydrolysis} \qquad \text{(Eq.20)}$$

$$HGR\ (\text{L}_{\text{H}_2}\ \text{min}^{-1}\ \text{g}_{\text{Cat}}^{-1}) = \frac{dP}{dt} \times \frac{V_{R_{Fin.}} V m_{STP}}{m_{Cat.} RT} \times 60 \qquad \text{(Eq.21)}$$

[4](born November, 1922 – die October, 2012) American inventor and scientist in the areas of energy and information.

4.1 Preliminary study

Most of studies about hydrogen generation by catalytic hydrolysis of sodium borohydride with a Ni-Ru based catalyst use a $NaBH_4$ amount of 1.2 g [4, 18, 21]. Although according to Eq. 1 the ideal hydrolysis reaction occurs for x=0, the best obtained results in this work thesis were for x=2 and a catalyst/$NaBH_4$ ratio of 0.2 g/g. Considering these facts, the first experiment was carried out with the same parameters that the other ones, but with 25 times less reactants. In order to verify the possibility of prevailing synergetic effect by increasing the total mass of reactants, a second experiment was performed with twice as much $NaBH_4$.

Both hydrogen generation curves, as initial parameters of first and second experiments, are represented in Figure 11 and Figure 12, respectively. The preliminary study results, such as yield, reaction rates and gravimetric and volumetric hydrogen densities, are presented in Table 6.

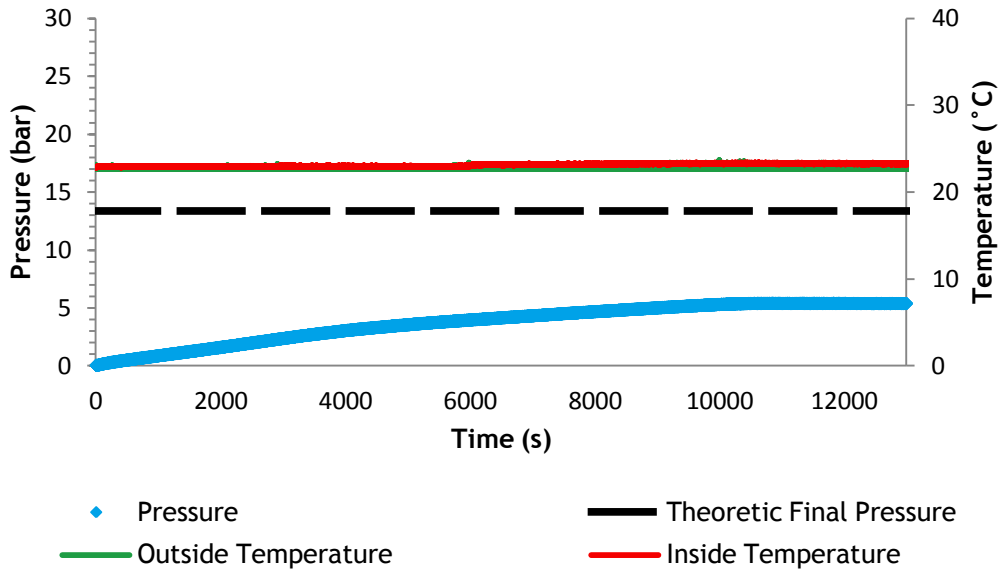

Figure 11| Hydrogen generation plot from the preliminary study. Conditions: m_{NaBH_4} = 0.0485 g; m_{Cat}/m_{NaBH_4} = 0.2 g/g; T = 22° C; x=2; catalyst 46x reused.

As expected, there is an increase in pressure along the experiment, which is compatible with H_2 generation. The H_2 yield was low (47.63%), probably due to a synergetic effect of $NaBH_4$. Moreover, inside and outside temperatures were constant and similar through the entire experiment, as highlighted by the graphic. This reflects the isolation capacity of the reactor, since there is no gain or loss of energy during the experiment.

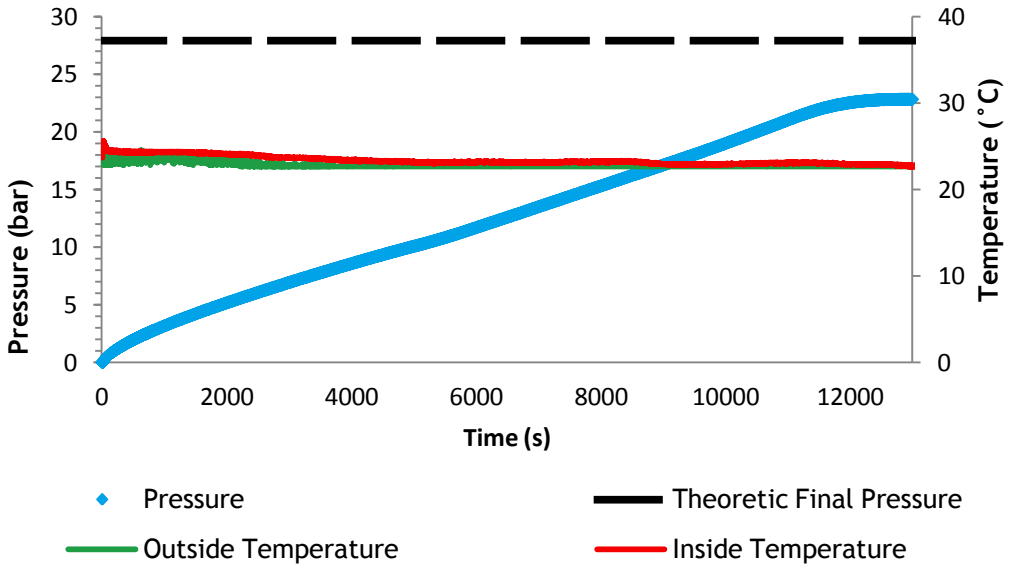

Figure 12| Hydrogen generation plot from the preliminary study. Conditions: m_{NaBH_4} = 0.1004 g; m_{Cat}/m_{NaBH_4} = 0.2 g/g; T = 22° C; *x*=2; catalyst 46x reused.

The graphic highlights an increase in pressure along the experiment, which is compatible with H_2 generation. The H_2 yield (85.46%) was higher than the one from the previous experiment (47.63%), proving the action of a synergetic effect of $NaBH_4$. Moreover, inside and outside temperatures were constant and similar through the entire experiment. This reflects the isolation capacity of the reactor, since there is no gain or loss of energy during the experiment.

Table 6| Preliminary study results.

m_{NaBH_4} (g)	η (%)	*dP/dt* (bar s^{-1})	HGR (L_{H_2} min^{-1} g_{Cat}^{-1})	GHSC (wt %)	VHSC (kg m^{-3})
0.0485	47.63	$7.00x10^{-4}$	0.04	2.71	28.86
0.1004	85.46	$3.30x10^{-3}$	0.09	5.46	58.13

* Calculated in STP conditions

Figures 11 and 12 reveal a notorious influence of the $NaBH_4$ available quantity at all levels. With the exception of the reaction duration, doubling the reactant weight amount induced the H_2 yield, reaction rates and storage capacities of approximately 2 times higher, as shown in Table 6. Taking this preliminary study into account, the following studies were performed with a $NaBH_4$ amount of, approximately, 0.1 g.

4.2 Effect of molar ratio $H_2O/NaBH_4$

Figures 13 to 18 show the course of hydrogen generation by changing the amount of $H_2O/NaBH_4$ ratio from 2 to 10 and also for 18 (mol/mol). As outlined in Figures 13 to 18, a catalyst/$NaBH_4$ ratio = 0.2 g/g was used in all experiments and the Ni-Ru based

catalyst was 47 times reused. As referred in section 2.2.2, the ideal hydrolysis is attained for *x*=0; however, increasing *x* will enhance the yield and accelerate the hydrogen generation rate [4], which is confirmed in the figures below.

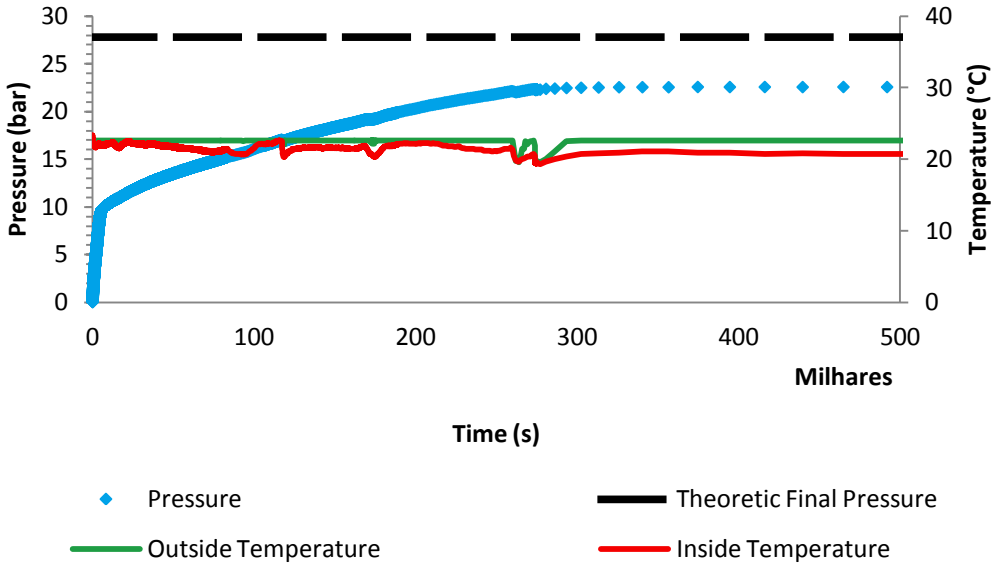

Figure 13|Hydrogen generation plot derived from $H_2O/NaBH_4$ molar ratio variation. Conditions: m_{NaBH_4} = 0.1004 g; m_{Cat}/m_{NaBH_4} = 0.2 g/g; T = 22° C; *x*=0; catalyst 47x reused.

The graphic representation reveals an increment of pressure along the experiment, with two different rates and a final H_2 yield of 84.57%. It is noteworthy the long duration of this experiment. The inside and outside temperatures were practically constant and similar through the entire reaction, corroborating the isolation of the reactor system.

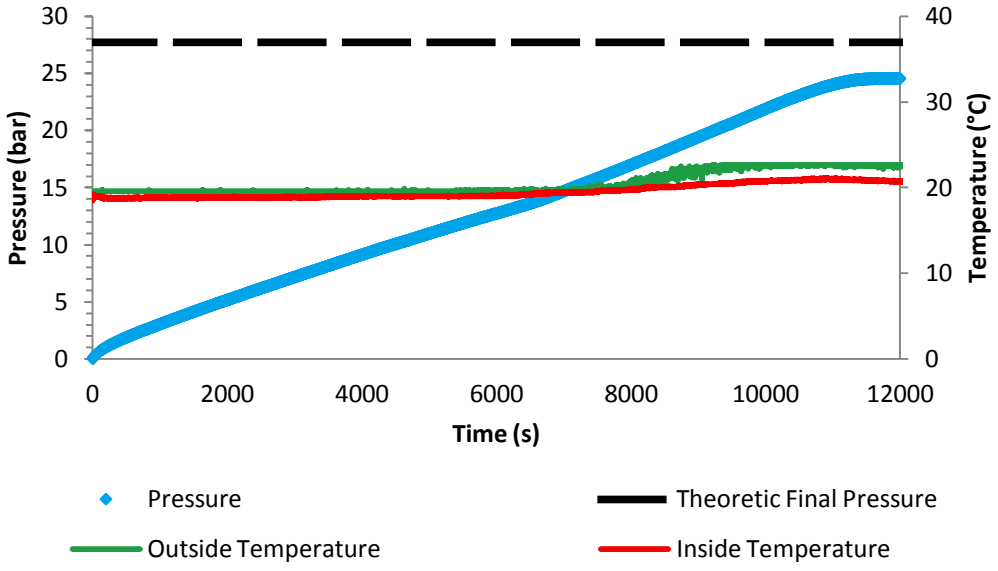

Figure 14| Hydrogen generation plot derived from $H_2O/NaBH_4$ molar ratio variation. Conditions: m_{NaBH_4} = 0.1004 g; m_{Cat}/m_{NaBH_4} = 0.2 g/g; T = 20° C; *x*=2; catalyst 47x reused.

Hydrogen generation was faster than in the previous experiment, as shown by the increment of pressure, with a final H_2 yield of 92.13%. The inside and outside temperatures were practically constant and similar through the entire reaction, corroborating the isolation of the reactor system.

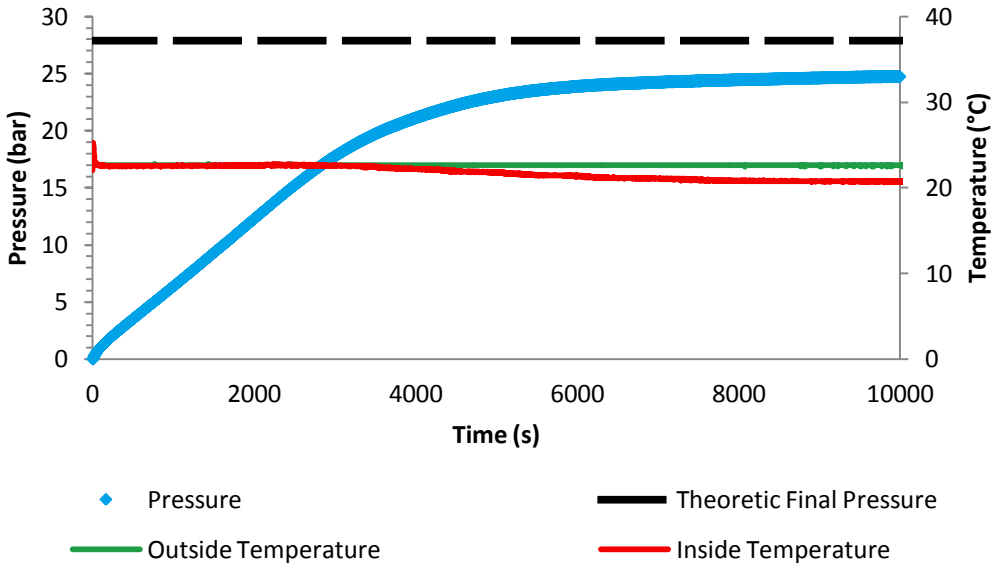

Figure 15| Hydrogen generation plot derived from $H_2O/NaBH_4$ molar ratio variation. Conditions: m_{NaBH_4} = 0.1003 g; m_{Cat}/m_{NaBH_4} = 0.2 g/g; T = 22° C; *x*=4; catalyst 47x reused.

The pressure increasing is concordant with hydrogen generation, which achieved a final H_2 yield of 92.40%. The inside and outside temperatures were practically constant and similar through the entire reaction, corroborating the isolation of the reactor system.

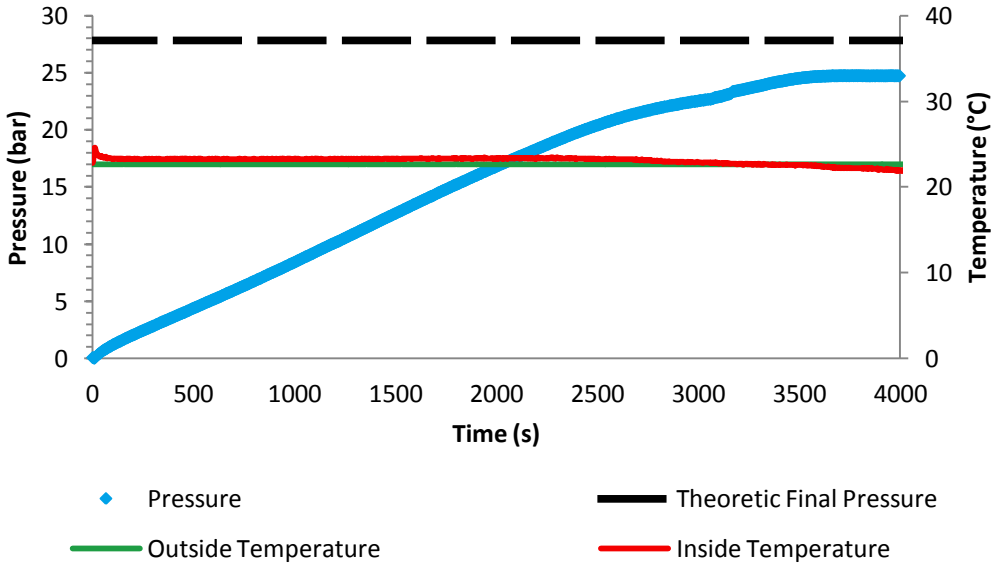

Figure 16| Hydrogen generation plot derived from $H_2O/NaBH_4$ molar ratio variation. Conditions: m_{NaBH_4} = 0.1001 g; m_{Cat}/m_{NaBH_4} = 0.2 g/g; T = 22° C; *x*=6; catalyst 47x reused.

The pressure increasing is concordant with hydrogen generation, and a final H_2 yield of 92.61% was achieved. Moreover, inside and outside temperatures were constant and similar through the entire experiment. This reflects the isolation capacity of the reactor, since there is no gain or loss of energy during the experiment.

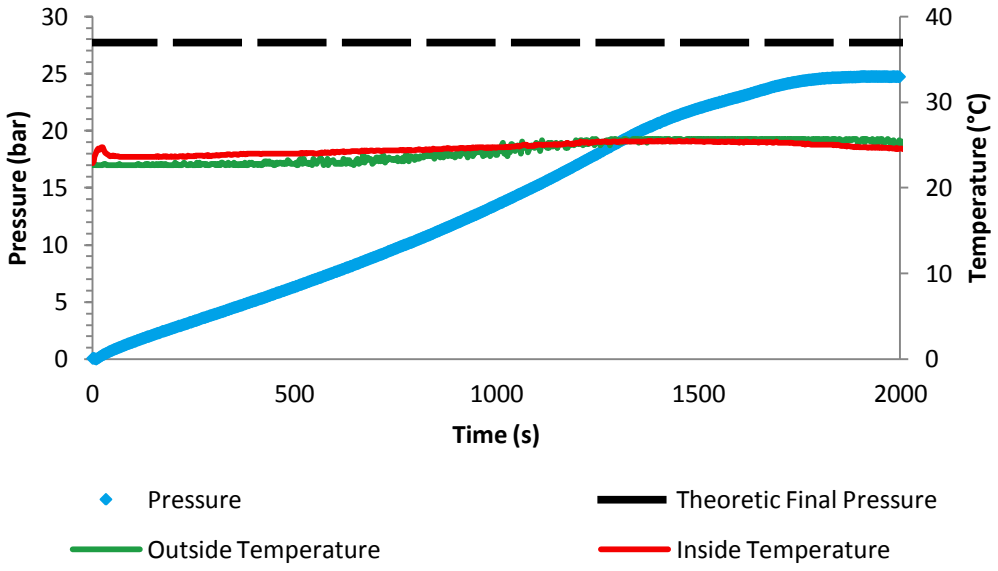

Figure 17| Hydrogen generation plot derived from $H_2O/NaBH_4$ molar ratio variation. Conditions: m_{NaBH_4} = 0.1000 g; m_{Cat}/m_{NaBH_4} = 0.2 g/g; T = 21° C; *x*=8; catalyst 47x reused.

The graphic highlights an increase in pressure along the experiment, which is compatible with H_2 generation with a yield rate of 92.61%. Moreover, inside and outside temperatures were constant and similar through the entire experiment. This reflects the isolation capacity of the reactor, since there is no gain or loss of energy during the experiment.

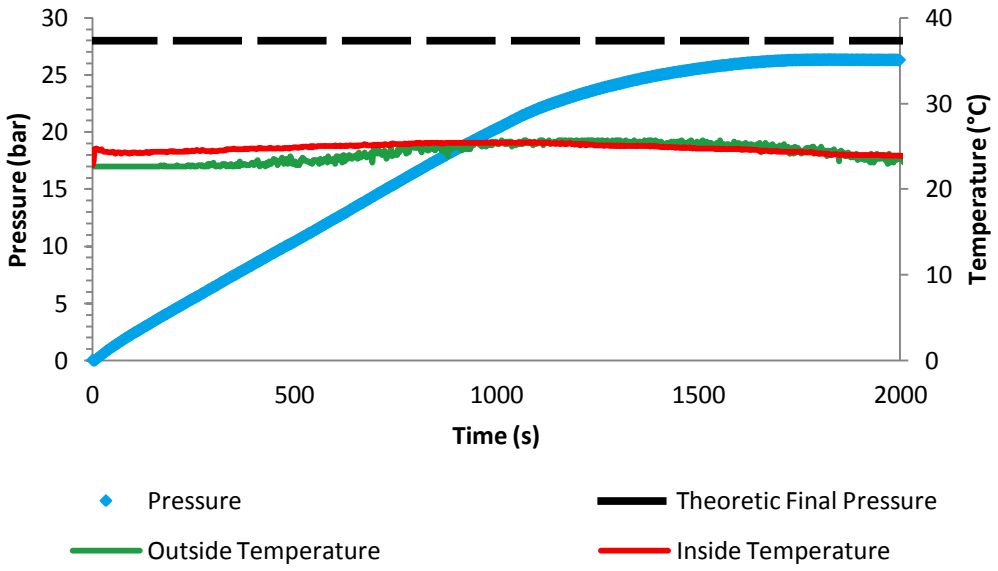

Figure 18| Hydrogen generation plot derived from $H_2O/NaBH_4$ molar ratio variation. Conditions: m_{NaBH_4} = 0.1005 g; m_{Cat}/m_{NaBH_4} = 0.2 g/g; T = 22° C; *x*=16; catalyst 47x reused.

The graphic highlights a faster pressure increase along the experiment. Thus, allowed to achieve a H_2 yield of 97.67%. Moreover, inside and outside temperatures were constant and similar through the entire experiment, as highlighted by the graphic. This reflects the isolation capacity of the reactor, since there is no gain or loss of energy during the experiment.

Kojima *et al*. (2004) [75] reported a hydrogen yield of about 80% after 400 s for the following conditions: x=0, catalyst$_{Pt\text{-}LiCoO_2}$/$NaBH_4$=0.5 g/g, at 6.8 bar and room temperature. Table 7 exhibit the results for the $H_2O/NaBH_4$ molar ratio studies and, for the same x value, the present work shows a similar yield of 84.57%, as referred by Kojima *et al*. (2004) [75]. Nevertheless, the ≈100 hours duration test (see Figure 17) is an undesirable factor. In any event, the 84.57% yield and 7.87 wt% H_2 are more rentable results than the ones obtained by Ferreira *et al*. (2010) [4] with a similar catalyst, in a reaction chamber with a conical bottom shape. Therefore, it can be claim that the reactor geometry may be a key factor in this working area.

Also, the x=16 experiment shows interesting results with high yield and hydrogen generation rate. However, the excess of water enhances borate solubility and, consequently, decreases the overall storage density [3]. Generation of hydrogen with high effective gravimetric and volumetric storage capacities is the utmost scientific challenges to overcome, before implementing an economy based on H_2. Thus, the ideal $H_2O/NaBH_4$ molar ratio boundaries should be comprised between $0 \leq x \leq 2$.

Table 7| Results obtained for $H_2O/NaBH_4$ molar ratio study, at room uncontrolled temperature.

x	η (%)	dP/dt (bar s^{-1})	HGR (L_{H_2} min^{-1} g_{Cat}^{-1})	GHSC (wt %)	VHSC (kg m^{-3})
0	84.57	1.80×10^{-3}	0.05	7.87	86.99
2	92.13	2.10×10^{-3}	0.06	5.82	62.20
4	92.40	5.70×10^{-3}	0.15	4.54	47.81
6	92.61	8.10×10^{-3}	0.22	3.69	38.45
8	92.95	1.73×10^{-2}	0.46	3.10	32.07
16	97.67	2.00×10^{-2}	0.53	2.00	20.41

* Calculated in STP conditions

4.3 Effect of catalyst/$NaBH_4$ mass ratio

Though catalyzed sodium borohydride hydrolysis requires excess of water to solid by-product hydration, an excess of water decreases the overall storage capacities [3]. Thus, all the experiments presented in this section were performed with a molar ratio $H_2O/NaBH_4$ = 2 mol/mol.

Comparing the plots of Figures 19 to 22 it can be highlighted that the amount of catalyst influences the rate of the hydrogen reaction and its lag time. Whenever the mass ratio of catalyst/$NaBH_4$ increases, faster the pressure attains its maximum, increasing *dP/dt* slope in the linear zone. However, as reported by Ferreira *et al.* (2010) [4], the hydrogen yield variation is negligible, despite the increasing catalyst/$NaBH_4$ mass ratio, as shown in Table 8. Although the positive increment on hydrogen generation rate, an increasing in the amount of catalyst is not viable. This increasing amount of catalyst would not achieve a comparable increment on the values of hydrogen yield and, consequently, in the hydrogen gravimetric density.

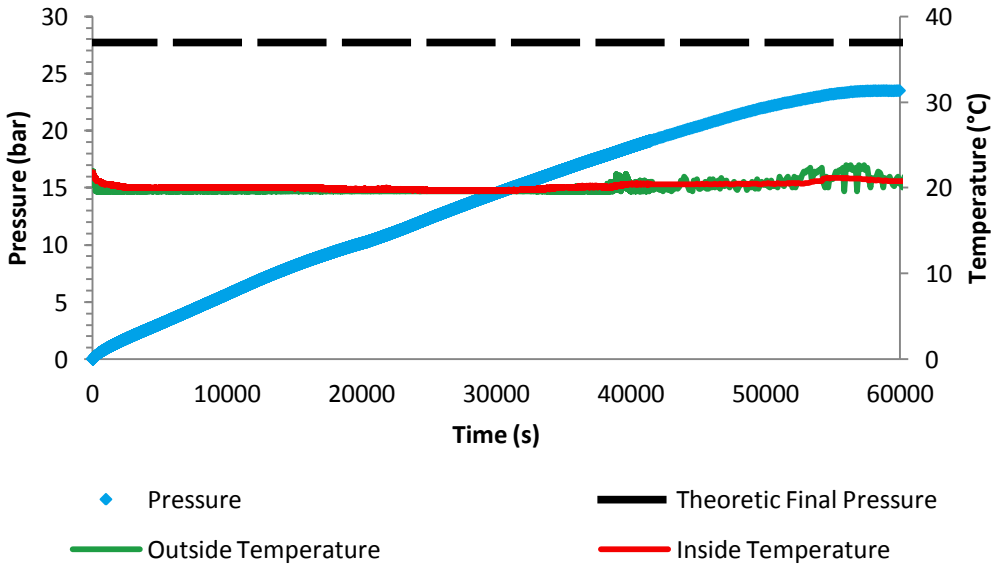

Figure 19| Hydrogen generation plot obtained from Catalyst/$NaBH_4$ mass ratio study. Conditions: m_{NaBH_4} = 0.1002 g; m_{Cat}/m_{NaBH_4} = 0.05 g/g; T = 21° C; *x*=2; catalyst 47x reused.

The increment of pressure with slow hydrogen generation rate is visible in the plot. The final H_2 yield obtained was 88.52%. The inside and outside temperatures were practically constant and similar through the entire reaction, corroborating the isolation of the reactor system.

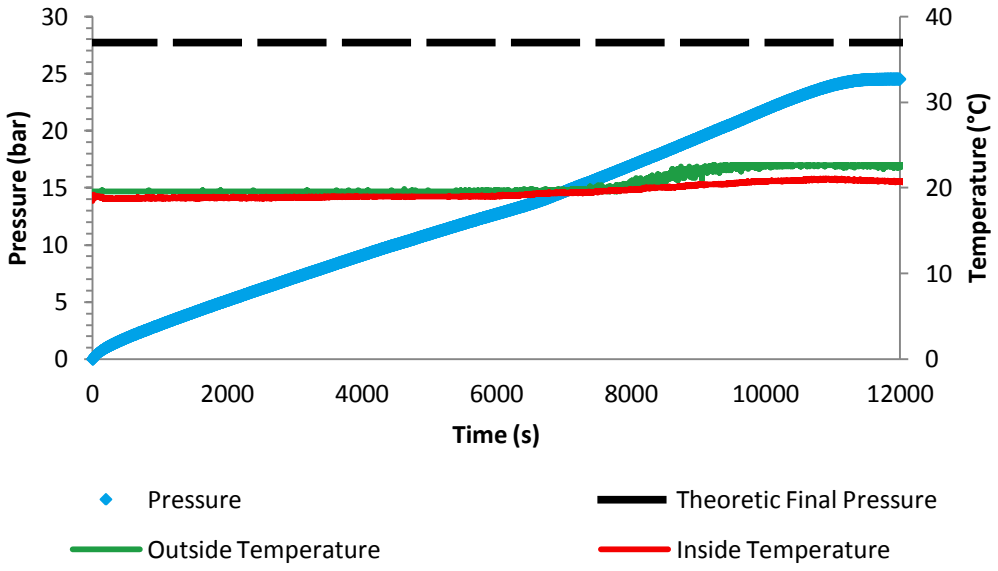

Figure 20| Hydrogen generation plot obtained from Catalyst/$NaBH_4$ mass ratio study. Conditions: m_{NaBH_4} = 0.1004 g; m_{Cat}/m_{NaBH_4} = 0.2 g/g; T = 20º C; *x*=2; catalyst 47x reused.

Hydrogen generation was faster than in the previous experiment, as shown by the increment of pressure, with a final H_2 yield of 92.13%. The inside and outside temperatures were practically constant and similar through the entire reaction, corroborating the isolation of the reactor system.

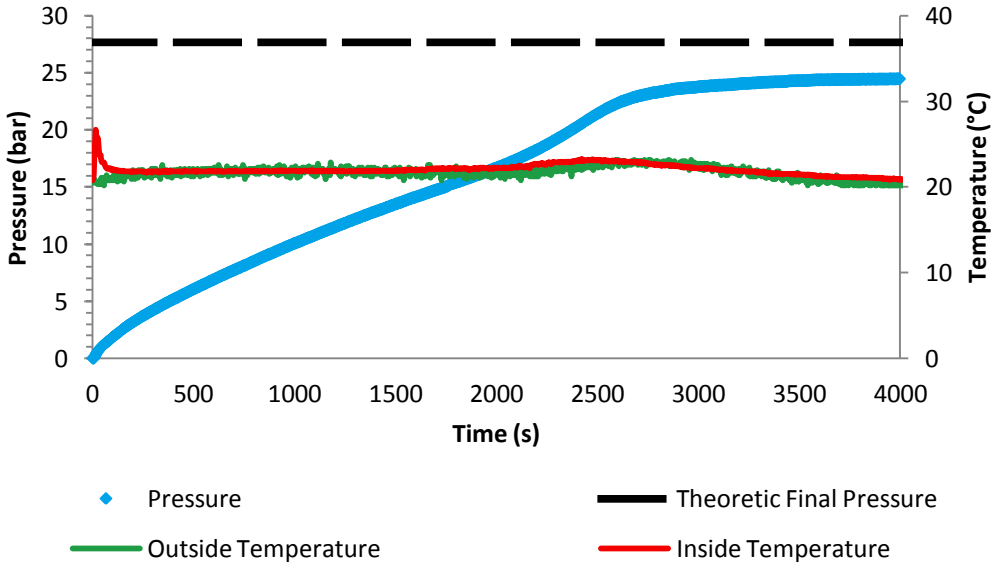

Figure 21| Hydrogen generation plot obtained from Catalyst/$NaBH_4$ mass ratio study. Conditions: m_{NaBH_4} = 0.1001 g; m_{Cat}/m_{NaBH_4} = 0.4 g/g; T = 20º C; *x*=2; catalyst 47x reused.

The pressure increasing is concordant with hydrogen generation, and a final H_2 yield of 92.34% was achieved. Moreover, it is visible an initial peak of inside temperature correspondent to an initial high H_2 generation rate. Nevertheless, outside temperature remain constant which reflects the isolation capacity of the reactor, since there is no gain or loss of energy during the experiment.

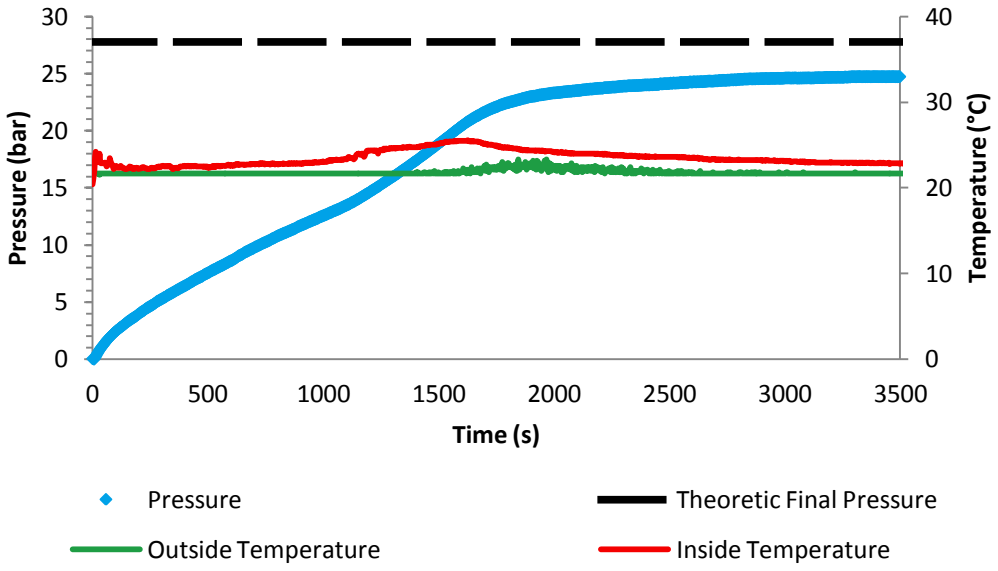

Figure 22| Hydrogen generation plot obtained from Catalyst/$NaBH_4$ mass ratio study. Conditions: m_{NaBH_4} = 0.1002 g; m_{Cat}/m_{NaBH_4} = 0.6 g/g; T = 21° C; *x*=2; catalyst 47x reused.

The plot shows the faster hydrogen generation rate of all catalyst/$NaBH_4$ mass ratio experiments. The final H_2 yield achieved was 92.66%. The inside and outside temperatures were practically constant and similar through the entire reaction, corroborating the isolation of the reactor system.

Table 8| Results obtained for catalyst/$NaBH_4$ mass ratio study, for $H_2O/NaBH_4$ = 4 mol/mol, at uncontrolled room temperature.

Catalyst/$NaBH_4$ (g/g)	η (%)	dP/dt (bar s^{-1})	HGR (L_{H_2} min^{-1} g_{Cat}^{-1})	GHSC (wt %)	VHSC (kg m^{-3})
0.05	88.52	4.00×10^{-4}	0.04	5.97	61.77
0.2	92.13	2.10×10^{-3}	0.06	5.82	62.20
0.4	92.34	1.04×10^{-2}	0.14	5.56	62.02
0.6	92.66	1.46×10^{-2}	0.13	5.28	61.14

* Calculated in STP conditions

4.4 Temperature effect

As stated in chapter 3.1.2, the Ni-Ru catalyst used in the experiments was optimized to work at 45°C. Therefore, it was expected that the studies performed with a higher temperature would enhance the catalyst behavior.

To evaluate the temperature influence in this work, three experiments with catalyst/$NaBH_4$ mass ratio of 0.2 g/g and $H_2O/NaBH_4$ molar ratio of 2, 4 and 18 mol/mol were carried out at controlled temperature of 55°C ± 5°C (at the beginning of the reaction the reactants temperature were not controlled). The results are represented in Figures 23-25, and exhibit an impressive increased rate reaction when

compared with similar tests, performed at uncontrolled room temperature (see Figures 13, 14 and 18).

The experiment performed for *x*=2 (see Figure 24) is noteworthy, due to the high hydrogen generation rate presented of 57.12 L min^{-1} g_{Cat}^{-1}, as shown in Table 9. This HGR value is, in fact, the highest value ever reported for the alkali free hydrolysis of $NaBH_4$ with a ruthenium based catalyst.

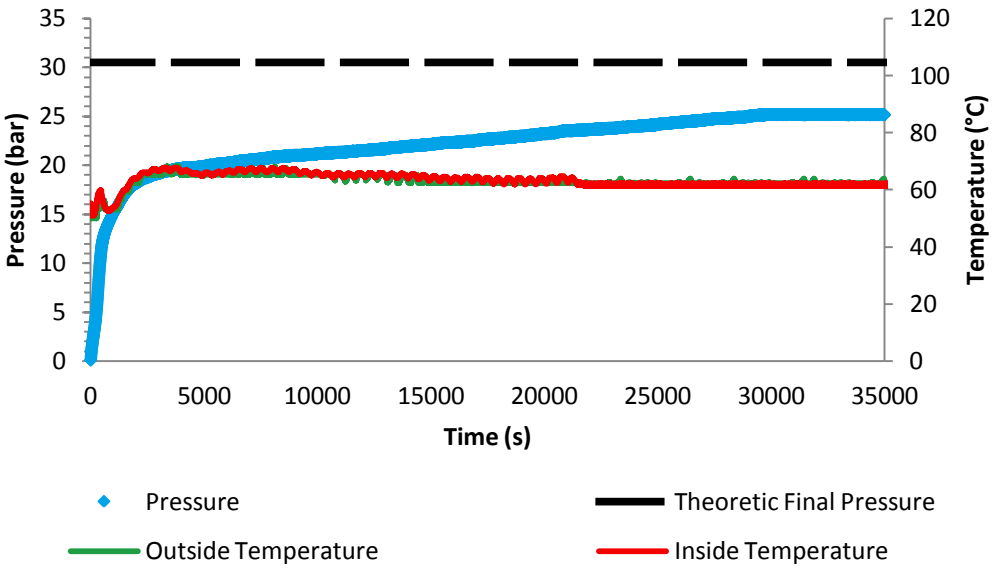

Figure 23| Hydrogen generation plot for $NaBH_4$ catalyzed hydrolysis at controlled temperature. Conditions: m_{NaBH_4} = 0.1003 g; m_{Cat}/m_{NaBH_4} = 0.2 g/g; T = 55° C; *x*=0; catalyst 48x reused.

The graphic representation reveals an increment of pressure along the experiment, with two different rates and a final H_2 yield of 84.60%. It is noteworthy the long duration of this experiment. With exception of the initial temperature peak - corresponding to an initial high H_2 generation rate - the inside and outside temperatures were practically constant and similar through the entire reaction, corroborating the isolation of the reactor system.

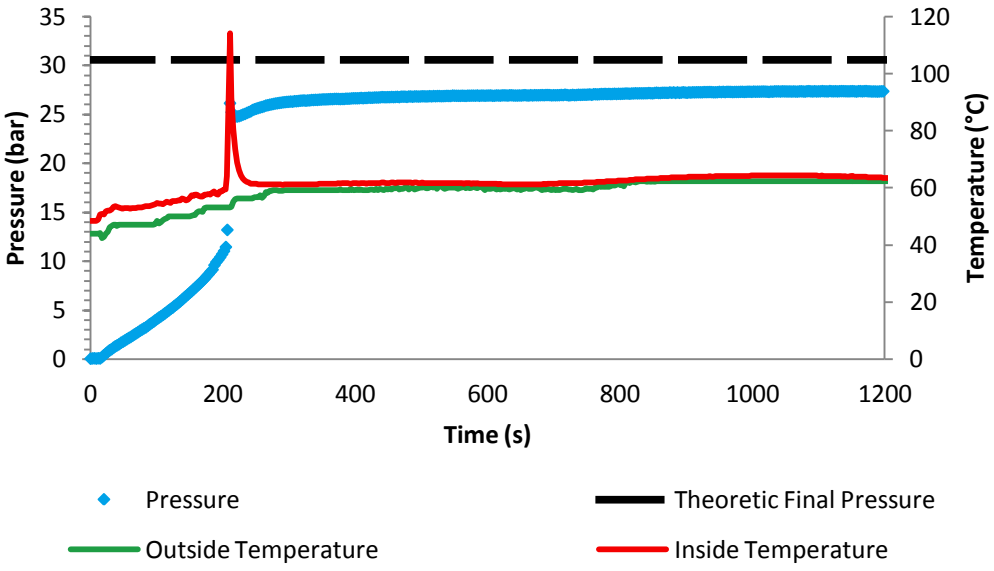

Figure 24| Hydrogen generation plot for $NaBH_4$ catalyzed hydrolysis at controlled temperature. Conditions: m_{NaBH_4} = 0.1003 g; m_{Cat}/m_{NaBH_4} = 0.2 g/g; T = 55° C; *x*=2; catalyst 48x reused.

The graphic representation present the higher H_2 generation rate of all studies, which is followed by a large peak from inside temperature. Nevertheless, outside temperature remains practically constant which reflects the isolation capacity of the reactor, since there is no gain or loss of energy during the experiment. A H_2 yield rate of 91.30% was obtained.

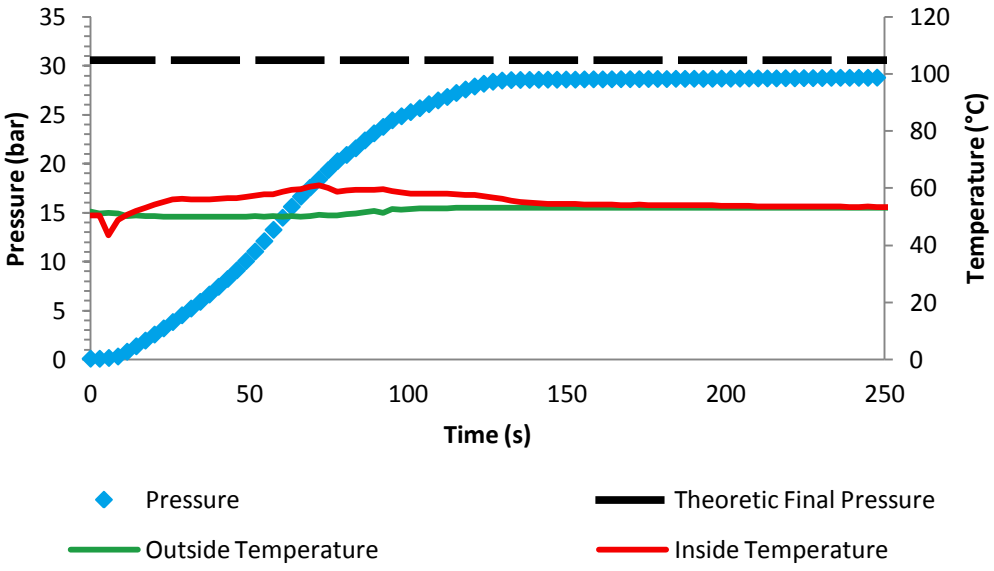

Figure 25| Hydrogen generation plot for $NaBH_4$ catalyzed hydrolysis at controlled temperature. Conditions: m_{NaBH_4} = 0.1003 g; m_{Cat}/m_{NaBH_4} = 0.2 g/g; T = 55° C; *x*=16; catalyst 48x reused.

The graphic highlights the faster increase in pressure of all studies, allowing obtaining 97.78% of H_2 yield. Moreover, inside and outside temperatures were constant and similar through the entire experiment. This reflects the isolation capacity of the reactor, since there is no gain or loss of energy during the experiment.

Also, the *x*=0 experiment (see Figure 23) presents a considerable time reduction in hydrogen generation when comparing with the results in Figure 13; nevertheless, this work thesis aimed to produce faster hydrogen gas, an energy carrier, without spending energy (heat, in this case). Moreover, the H_2 yield was similar between the experiments performed at controlled temperature (55 ± 5°C) and at room uncontrolled temperature (20-25 °C). Thus, the use of sodium borohydride hydrolysis at controlled high temperature is not profitable, since the dispended energy, to increase the reaction medium temperature, does not compensates the hydrogen generation yields. Therefore, the synthesis of a catalyst capable of inducing a high generation rate, at room temperature, is required and crucial to implement an economy based on H_2.

Table 9| Results of the study of the influence of temperature.

x	Temperature (°C)	*η* (%)	*dP/dt* (bar s^{-1})	HGR (L_{H_2} min^{-1} g_{Cat}^{-1})	GHSC (wt %)	VHSC (kg m^{-3})
0	22	84.57	1.80×10^{-3}	0.05	7.87	86.99
	55	84.60	3.14×10^{-2}	0.76	7.90	86.83
2	20	92.13	2.10×10^{-3}	0.06	5.82	62.20
	55	91.30	2.37	57.12	5.88	62.52
16	22	97.67	2.00×10^{-2}	0.53	2.00	20.41
	55	97.78	3.30×10^{-1}	7.94	2.00	20.31

* Calculated in STP conditions

4.5 Alkali hydrolysis

To assess the influence of NaOH inhibitor, the experiments were performed under the following conditions: x=16, catalyst/$NaBH_4$ = 0.2 g/g and NaOH concentration of 1% and 7% by weight. Figures 26 and 27, shows the NaOH effect on hydrogen generation curves.

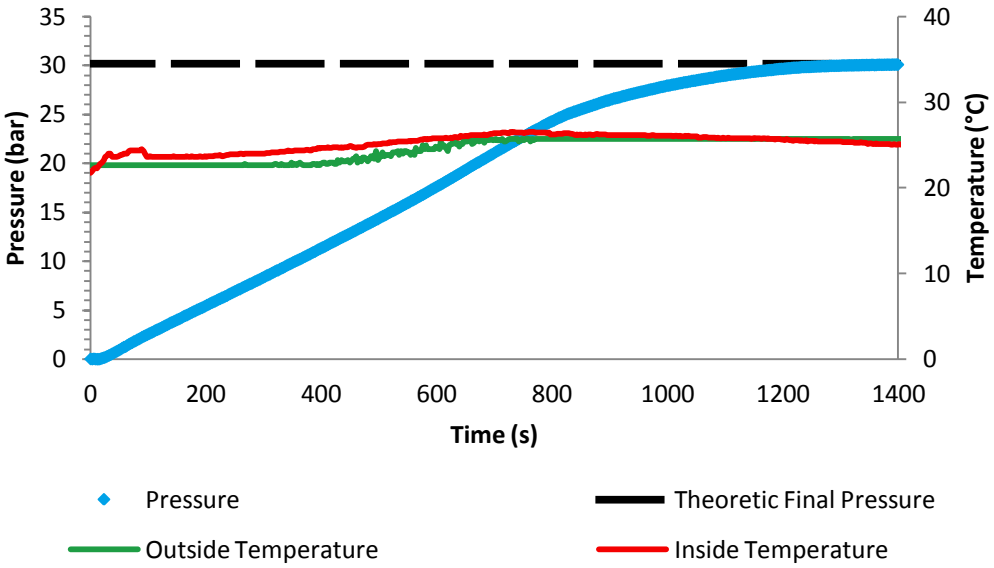

Figure 26| Hydrogen generation plot from alkali hydrolysis study. Conditions: m_{NaBH_4} = 0.1087 g; m_{Cat}/m_{NaBH_4} = 0.2 g/g; 1 wt% NaOH ; T = 21° C; *x*=16; catalyst 47x reused.

The graphic represented shows an increasing of pressure that allowed achieving 100% on H_2 yield rate. The inside and outside temperatures were practically constant and similar through the entire reaction, corroborating the isolation of the reactor system.

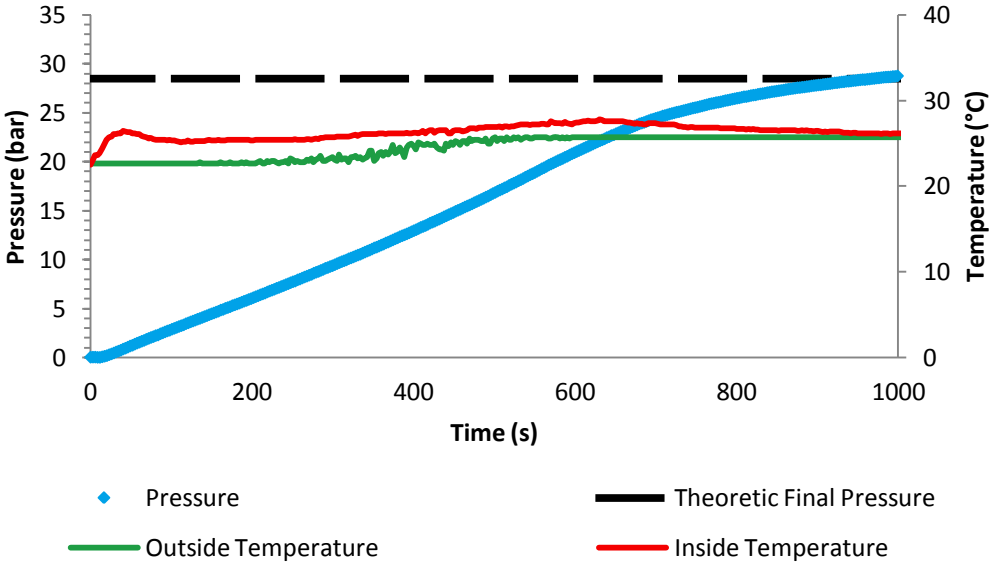

Figure 27| Hydrogen generation plot from alkali hydrolysis study. Conditions: m_{NaBH_4} = 0.1029 g; m_{Cat}/m_{NaBH_4} = 0.2 g/g; 7 wt% NaOH ; T = 21° C; *x*=16; catalyst 47x reused.

As well as previous plot, a 100% H_2 yield was achieved. The graphic represented reveals that the inside and outside temperatures were practically constant and similar through the entire reaction, corroborating the isolation of the reactor system.

As reported by Hua *et al.* (2003) [36], which use a nickel boride catalyst, the presence of NaOH inhibitor not only enhances the reaction rate but also increases the H_2 yield to 100%, which means that the reaction was fully completed.

The results for the $NaBH_4$ alkali hydrolysis study are represented in Table 10.

Table 10| Results obtained for $NaBH_4$ alkali hydrolysis study for $H_2O/NaBH_4$ = 18 mol/mol, at uncontrolled room temperature.

NaOH (wt %)	η (%)	dP/dt (bar s^{-1})	HGR (L_{H_2} min^{-1} g_{Cat}^{-1})	GHSC (wt %)	VHSC (kg m^{-3})
0	97.67	2.00×10^{-2}	0.53	2.00	20.41
1	100	3.11×10^{-2}	0.81	2.14	21.90
7	100	3.95×10^{-2}	1.02	2.29	23.40

* Calculated in STP conditions

4.6 Activation energy study

As referred in Chapter 4.4, temperature plays a vital role in hydrogen generation process, i.e. HGR increases as the temperature increases. Therefore, to characterize the Ni-Ru catalyst activity after 48 reutilizations, experiments were performed at different temperatures. Figure 28 shows the hydrogen generation, in terms of H_2 pressure as a function of time, using constants molar ratio $H_2O/NaBH_4$ (4 mol/mol) and mass ratio catalyst/$NaBH_4$ (0.2 g/g) at 20ºC, 45ºC and 55ºC.

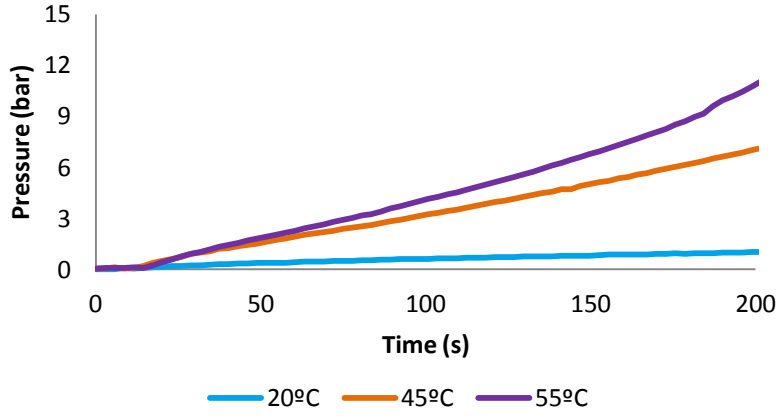

Figure 28| Hydrogen generation rate as a function of time, at different temperatures. Conditions: m_{NaBH_4} ≈ 0.1000 g; m_{Cat}/m_{NaBH_4} = 0.2 g/g; *x*=2; catalyst 48x reused.

The plot shows that increasing temperature gave rise to higher H_2 production rates. The catalytic sodium borohydride hydrolysis at 55ºC had a higher HGR than the one at 45ºC, which, in turn, had a higher HGR than the one at 20ºC.

In order to estimate the catalyst activation energy (*E*) the Arrhenius plot of ln*k* vs. 1/*T* were represented (Figure 29), where *k* is the reaction rate. The activation energy is 75.12 kJ mol^{-1}, as calculated from the slope of the fitted straight line in Figure 29. As shown in Table 4, the activation energy obtained is one of the highest reported for a Ru based catalyst.

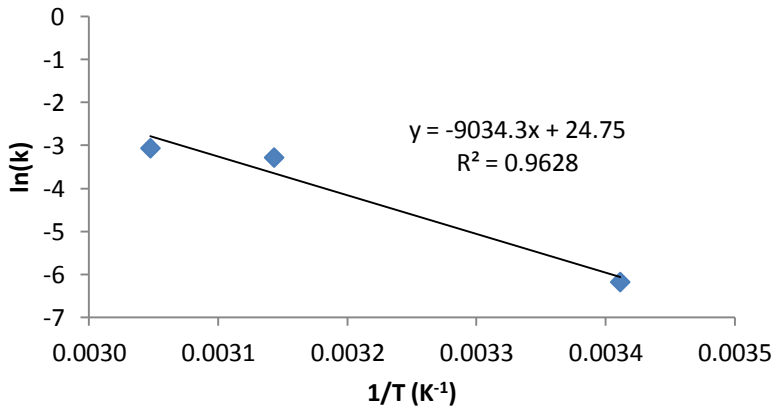

Figure 29| Arrhenius plot obtained from the kinetic data of hydrolysis reaction performed at temperatures: 20°C, 45°C and 55°C.

4.7 Open literature comparison

Ferreira *et al*. (2012) [18] reported the role of reactor bottom geometry for hydrogen generation and storage by solid sodium borohydride hydrolysis. Figures 30 and 31 illustrate the influence of the molar ratio $H_2O/NaBH_4$ on H_2 yield and GHSC, respectively, with the results obtained by Ferreira *et al*. (2012) [18] for comparison.

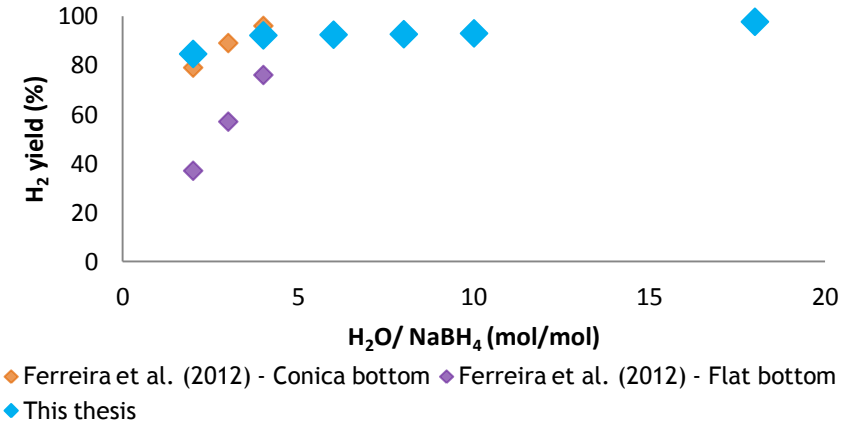

Figure 30| Hydrogen generation yields as a function of added water, performed at room temperature with a mass ratio catalyst/$NaBH_4$ = 0.2 g/g.

The plot emphasis the importance of the reactor bottom geometry on the optimization of $NaBH_4$ hydrolysis reaction. Moreover, it is visible that, for the ovoid shape reactor, increasing the water amount does not increase the H_2 yield significantly.

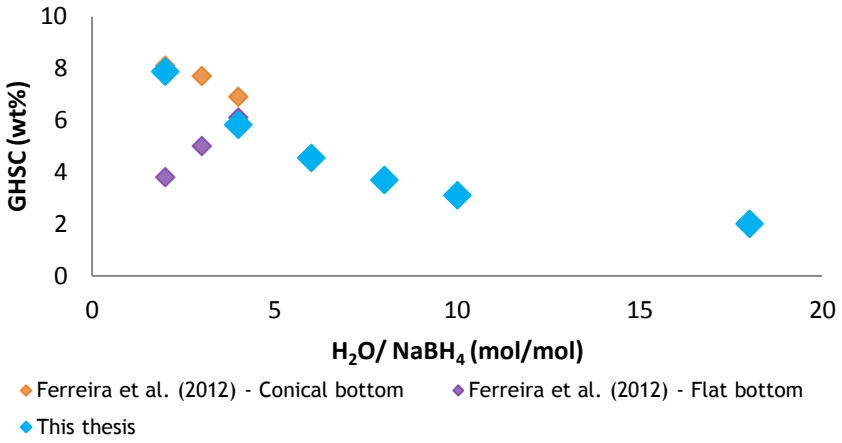

Figure 31| Gravimetric hydrogen storage capacity as a function of added water, performed at room temperature with a mass ratio catalyst/$NaBH_4$ = 0.2 g/g.

Again, the importance of the reactor bottom geometry on the optimization of $NaBH_4$ hydrolysis reaction is evident. Furthermore, the ideal hydrolysis ($H_2O/NaBH_4$ = 2 mol/mol) shows the highest GHSC for both conical and ovoid geometries.

Figure 30 allows observing that H_2 yield increases with increasing $H_2O/NaBH_4$ molar ratio. The H_2 yield rates obtained from egg-shaped mini reactor are similar to the ones obtained from conical bottom geometry. Moreover, for the ideal hydrolysis reaction (x=0), both geometries presents a H_2 yield rates more than 2 times higher than the corresponding values in flat bottom reactor.

Figure 31 presents the highest effective value for GHSC (8.10 wt%) on a material only basis, obtained from Ferreira *et al.* (2012) [18]. However, the novel mini-reactor presents a similar value (7.87 wt%) at equal conditions.

Both Figures 30 and 31 show that, with ideal hydrolysis (x=0), the reactor geometry strongly influences the H2 generated yields and rates and enhanced the energy densities.

Catalytic sodium borohydride hydrolysis with $H_2O/NaBH_4$ = 2 mol/mol to produce anhydrous sodium borate, or less hydrate by-products, is the key to increase the overall storage density capacities. Considering this, the plot in Figure 32 shows the hydrogen generation yield versus pressure, for the stoichiometric amount of water $H_2O/NaBH_4$ = 2 mol/mol, at uncontrolled room temperature. Also the results obtained by Kojima *et al.* (2004) [75] and Ferreira *et al.* (2012) [18].

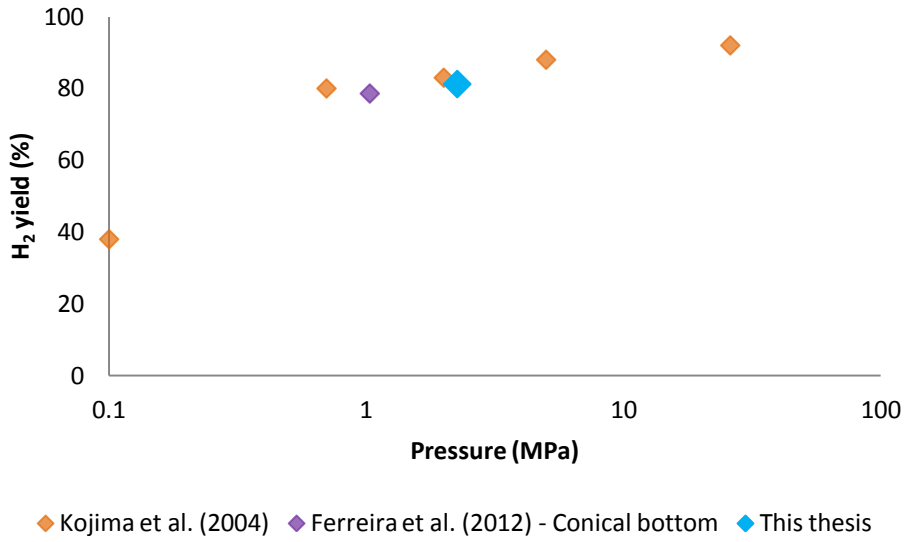

Figure 32| Influence of pressure on hydrogen yield excluding any excess of water, at room temperature.

The representation reveals an increment in H_2 yield as the pressure increases. Moreover, for a lower amount of catalyst, the conical and ovoid reactor geometries allow achieving similar results at moderate pressure.

As seen in Figure 32, the effect of the reactor geometry and the operating pressure on hydrogen yield is notable, i.e. increasing the pressure, significantly increases hydrogen yields. Kojima *et al.* (2004) [75] reported values of 80-93% for hydrogen yields under higher pressure levels (0.7-25 MPa) using a mass ratio $catalyst_{PtLiCoO_2}/NaBH_4$ = 0.5 g/g. Ferreira *et al.* (2012) [18] reported a value of 79% for hydrogen yield at the moderate pressure of 1.0 MPa with a $catalyst_{Ni\text{-}Ru}/NaBH_4$ = 0.2 g/g. For the particular case of the present work, at the moderate pressure of 2.3 MPa, a value of 81.23% for hydrogen yield was obtained using Ni-Ru based powdered catalyst (catalyst/$NaBH_4$ = 0.2 g/g), reused 47 times, which shows high activity under moderate pressure.

5 Conclusions

"Hydrogen is a small atom. However, it will play an important role in future energy." Günther Öttinger[5]

Aiming to develop the ideal geometry of a reactor for hydrogen generation and storage for portable applications, an innovator egg-shaped mini-reactor was built. To ensure its applicability, several sodium borohydride catalyzed hydrolysis studies were performed, to assess temperature and inhibitor influence, as well as water and catalyst amount effects. As described in literature, increasing the $H_2O/NaBH_4$ molar ratio increases the yield and hydrogen generation rates and considerably diminishes the gravimetric and volumetric storage capacities. It is noteworthy that these storage capacities are only influenced by the $H_2O/NaBH_4$ molar ratio. The catalyst/$NaBH_4$ mass ratio only influenced the hydrogen generation rate, which is higher as the ratio increases. According to literature, it would also be expected an increment in yield rate; although this increment was visible, it was not significant. Similar results were obtained for the temperature effect studies, with the exception of the yield rate, which not always increased. Nevertheless, it should be highlighted the highest hydrogen generation rate ever reported for alkali free hydrolysis of $NaBH_4$ with a nickel-ruthenium based catalyst (57.12 L_{H_2} min^{-1} g_{Cat}^{-1}).

From alkali hydrolysis studies, it could be concluded that the presence of the NaOH inhibitor enhanced the yield and hydrogen generation rates. Independently of the NaOH amount (1 wt% and 7 wt%), a yield of 100% was achieved, indicating the completeness of the hydrolysis reaction.

In order to characterize the catalyst activity, after 48 reutilizations, the activation energy was calculated. The value of 75.12 kJ mol^{-1} was obtained for a range of temperatures of 20-55ºC.

Finally, the results obtained from this thesis were compared with the open literature which allows reinforcing the importance of the reactor geometry in the "ideal" catalytic sodium borohydride hydrolysis (x=0).

In summary, it can be concluded that the ovoid geometry of the mini-reactor was suitable for an efficient hydrogen generation by sodium borohydride catalyzed hydrolysis capable of adoption for on demand H2-PEMFC in portable applications.

[5](born October, 1953) European Commissioner for Energy in the European Commission since February 2010.

5.1 Future work and perspectives

This work has provided important insights about the role of reactor geometry on hydrogen generation and storage by sodium borohydride hydrolysis. Future studies should be conducted in order to discover new materials that support the construction of a lighter reactor, such as engineering polymers. This achievement is crucial, since the obtained results do not fulfill the ultimate requirements of US DOE for a material only basis hydrogen storage capacity.

Furthermore, the synthesis of a suitable catalyst that mimics, at room temperature (≈22ºC), the behavior of the one used in this thesis at controlled high temperature (55 ± 5ºC). Moreover other metal catalysts should be researched to improve the sodium borohydride catalyzed hydrolysis reaction. These catalysts could possibly allow the improvement not only of the reaction rates, but also the overall storage capacities.

Also the kinetics for sodium borohydride hydrolysis should be studied, since it is important to develop a kinetic model that reflects the reaction as a function of concentration, pressure and temperature for the novel mini-reactor.

Moreover it is essential to close the loop of the reaction by studding the by-products ($NaBO_2 \bullet xH_2O$) and found a method to recycling them back to sodium borohydride.

Given the crescent necessity of a green economy, the data obtained from this work may provide novel insights to establish a hydrogen based economy for portable applications.

6 Bibliography

"The two most common elements in the universe are hydrogen and stupidity."
Harlan Ellison[6]

[1] V. Fernandes, "Characterisation of materials for hydrogen storage," M.Phil. Thesis, University of Manchester, 2010.

[2] S. Amendola, "A safe, portable, hydrogen gas generator using aqueous borohydride solution and Ru catalyst," *Int. J. Hydrogen Energy*, vol. 25, no. 10, pp. 969–975, Oct. 2000.

[3] U. B. Demirci, O. Akdim, J. Andrieux, J. Hannauer, R. Chamoun, and P. Miele, "Sodium Borohydride Hydrolysis as Hydrogen Generator: Issues, State of the Art and Applicability Upstream from a Fuel Cell," *Fuel Cells*, vol. 10, no. 3, pp. 335–350, Jun. 2010.

[4] M. J. F. Ferreira, L. Gales, V. R. Fernandes, C. M. Rangel, and A. M. F. R. Pinto, "Alkali free hydrolysis of sodium borohydride for hydrogen generation under pressure," *Int. J. Hydrogen Energy*, vol. 35, no. 18, pp. 9869–9878, Sep. 2010.

[5] C. R. Cloutier, "Electrochemical recycling of sodium borohydride for hydrogen storage: Physicochemical properties of sodium metaborate solutions," M.S. Thesis, University of British Columbia, 2006.

[6] D. Kılınç, C. Saka, and Ö. Şahin, "Hydrogen generation from catalytic hydrolysis of sodium borohydride by a novel Co(II)–Cu(II) based complex catalyst," *J. Power Sources*, vol. 217, pp. 256–261, Nov. 2012.

[7] F. Barbir, "Transition to renewable energy systems with hydrogen as an energy carrier," *Energy*, vol. 34, no. 3, pp. 308–312, Mar. 2009.

[8] A. Ajanovic, "Renewable fuels – A comparative assessment from economic, energetic and ecological point-of-view up to 2050 in EU-countries," *Renew. Energy*, vol. 60, pp. 733–738, Dec. 2013.

[9] F. M. Orr Jr., T. S. Ramakrishnan, C. Roulet, and E. Stout, "Hydrogen: A Future Energy Carrier ?," *Oilfield Review*, pp. 30–41, 2005.

[10] M. J. F. Ferreira, "Catalytic generation and storage of hydrogen from hydrolysis of sodium-borohydride under pressure," M.S. Thesis, Faculty of Engineering from University of Porto, 2009.

[11] S. S. Muir and X. Yao, "Progress in sodium borohydride as a hydrogen storage material: Development of hydrolysis catalysts and reaction systems," *Int. J. Hydrogen Energy*, vol. 36, no. 10, pp. 5983–5997, May 2011.

[6](born May, 1934) American writer.

[12] K. Mazloomi and C. Gomes, "Hydrogen as an energy carrier: Prospects and challenges," *Renew. Sustain. Energy Rev.*, vol. 16, no. 5, pp. 3024–3033, Jun. 2012.

[13] US Department of Energy, "A national vision of America's transition to a hydrogen economy to 2030 and beyond," Washington DC, 2002.

[14] European Comission, *Introducing Hydrogen as an energy carrier*. Luxembourg: Office for Official Publications of the European Communities, 2006, p. 40.

[15] U. B. Demirci and P. Miele, "Sodium tetrahydroborate as energy/hydrogen carrier, its history," *Comptes Rendus Chim.*, vol. 12, no. 9, pp. 943–950, Sep. 2009.

[16] M. J. F. Ferreira, F. Coelho, C. M. Rangel, and a. M. F. R. Pinto, "Batch sodium borohydride hydrolysis systems: Effect of sudden valve opening on hydrogen generation rate," *Int. J. Hydrogen Energy*, vol. 37, no. 2, pp. 1947–1953, Jan. 2012.

[17] U. D. of Energy, "Targets for Onboard Hydrogen Storage Systems for Light-Duty Vehicles," 2009.

[18] M. J. F. Ferreira, C. M. Rangel, and a. M. F. R. Pinto, "Water handling challenge on hydrolysis of sodium borohydride in batch reactors," *Int. J. Hydrogen Energy*, vol. 37, no. 8, pp. 6985–6994, Apr. 2012.

[19] M. J. F. Ferreira, V. R. Fernandes, L. Gales, C. M. Rangel, and A. M. F. R. Pinto, "Effects of the addition of an organic polymer on the hydrolysis of sodium tetrahydroborate in batch reactors," *Int. J. Hydrogen Energy*, vol. 35, no. 20, pp. 11456–11469, Oct. 2010.

[20] U.S. Department of Energy, "Energy Efficiency & Renewable Energy," *Status of Hydrogen Storage Technologies*, 2009. [Online]. Available: http://www1.eere.energy.gov/hydrogenandfuelcells/storage/tech_status.html. [Accessed: 24-Jan-2014].

[21] M. J. F. Ferreira, C. M. Rangel, and A. M. F. R. Pinto, "Batch solid sodium borohydride hydrolysis for hydrogen generation: The role of reactor bottom shape," in *4th World Hydrogen Technologies Convention*, 2011, pp. 2–7.

[22] C.-C. Yang, M.-S. Chen, and Y.-W. Chen, "Hydrogen generation by hydrolysis of sodium borohydride on CoB/SiO2 catalyst," *Int. J. Hydrogen Energy*, vol. 36, no. 2, pp. 1418–1423, Jan. 2011.

[23] C.-W. Chen, C.-Y. Chen, and Y.-H. Huang, "Method of preparing Ru-immobilized polymer-supported catalyst for hydrogen generation from NaBH4 solution," *Int. J. Hydrogen Energy*, vol. 34, no. 5, pp. 2164–2173, Mar. 2009.

[24] H. I. Schlesinger, H. C. Brown, A. E. Finholt, J. R. Gilbreath, H. R. Hoekstra, and E. K. Hyde, "Sodium Borohydride, Its Hydrolysis and its Use as a Reducing Agent and in the Generation of Hydrogen," *J. Am. Chem. Soc.*, vol. 75, no. 1, pp. 215–219, Jan. 1953.

[25] B. H. Liu, Z. P. Li, and S. Suda, "Nickel- and cobalt-based catalysts for hydrogen generation by hydrolysis of borohydride," *J. Alloys Compd.*, vol. 415, no. 1–2, pp. 288–293, May 2006.

[26] C.-H. Liu, B.-H. Chen, C.-L. Hsueh, J.-R. Ku, M.-S. Jeng, and F. Tsau, "Hydrogen generation from hydrolysis of sodium borohydride using Ni–Ru nanocomposite as catalysts," *Int. J. Hydrogen Energy*, vol. 34, no. 5, pp. 2153–2163, Mar. 2009.

[27] Y. generation from hydrolysis of sodium borohydride using N. nanocomposite as catalysts Liang, H.-B. Dai, L.-P. Ma, P. Wang, and H.-M. Cheng, "Hydrogen generation from sodium borohydride solution using a ruthenium supported on graphite catalyst," *Int. J. Hydrogen Energy*, vol. 35, no. 7, pp. 3023–3028, Apr. 2010.

[28] S. U. Jeong, R. K. Kim, E. a. Cho, H.-J. Kim, S.-W. Nam, I.-H. Oh, S. -a. Hong, and S. H. Kim, "A study on hydrogen generation from NaBH4 solution using the high-performance Co-B catalyst," *J. Power Sources*, vol. 144, no. 1, pp. 129–134, Jun. 2005.

[29] C. Wu, F. Wu, Y. Bai, B. Yi, and H. Zhang, "Cobalt boride catalysts for hydrogen generation from alkaline NaBH4 solution," *Mater. Lett.*, vol. 59, no. 14–15, pp. 1748–1751, Jun. 2005.

[30] J. C. Walter, A. Zurawski, D. Montgomery, M. Thornburg, and S. Revankar, "Sodium borohydride hydrolysis kinetics comparison for nickel, cobalt, and ruthenium boride catalysts," *J. Power Sources*, vol. 179, no. 1, pp. 335–339, Apr. 2008.

[31] H.-B. Dai, Y. Liang, P. Wang, and H.-M. Cheng, "Amorphous cobalt–boron/nickel foam as an effective catalyst for hydrogen generation from alkaline sodium borohydride solution," *J. Power Sources*, vol. 177, no. 1, pp. 17–23, Feb. 2008.

[32] P. Krishnan, S. G. Advani, and A. K. Prasad, "Thin-film CoB catalyst templates for the hydrolysis of NaBH4 solution for hydrogen generation," *Appl. Catal. B Environ.*, vol. 86, no. 3–4, pp. 137–144, Feb. 2009.

[33] H. Dai, Y. Liang, P. Wang, X. Yao, T. Rufford, M. Lu, and H. Cheng, "High-performance cobalt–tungsten–boron catalyst supported on Ni foam for hydrogen generation from alkaline sodium borohydride solution," *Int. J. Hydrogen Energy*, vol. 33, no. 16, pp. 4405–4412, Aug. 2008.

[34] D.-W. Zhuang, J.-J. Zhang, H.-B. Dai, and P. Wang, "Hydrogen generation from hydrolysis of solid sodium borohydride promoted by a cobalt–molybdenum–boron catalyst and aluminum powder," *Int. J. Hydrogen Energy*, vol. 38, no. 25, pp. 10845–10850, Aug. 2013.

[35] J. C. Ingersoll, N. Mani, J. C. Thenmozhiyal, and A. Muthaiah, "Catalytic hydrolysis of sodium borohydride by a novel nickel–cobalt–boride catalyst," *J. Power Sources*, vol. 173, no. 1, pp. 450–457, Nov. 2007.

[36] D. Hua, “Hydrogen production from catalytic hydrolysis of sodium borohydride solution using nickel boride catalyst,” *Int. J. Hydrogen Energy*, vol. 28, no. 10, pp. 1095–1100, Oct. 2003.

[37] Y. Chen and H. Kim, “Use of a nickel-boride–silica nanocomposite catalyst prepared by in-situ reduction for hydrogen production from hydrolysis of sodium borohydride,” *Fuel Process. Technol.*, vol. 89, no. 10, pp. 966–972, Oct. 2008.

[38] N. Malvadkar, S. Park, M. Urquidi-MacDonald, H. Wang, and M. C. Demirel, “Catalytic activity of cobalt deposited on nanostructured poly(p-xylylene) films,” *J. Power Sources*, vol. 182, no. 1, pp. 323–328, Jul. 2008.

[39] J.-H. Kim, H. Lee, S.-C. Han, H.-S. Kim, M.-S. Song, and J.-Y. Lee, “Production of hydrogen from sodium borohydride in alkaline solution: development of catalyst with high performance,” *Int. J. Hydrogen Energy*, vol. 29, no. 3, pp. 263–267, Mar. 2004.

[40] Ö. Metin and S. Özkar, “Hydrogen generation from the hydrolysis of sodium borohydride by using water dispersible, hydrogenphosphate-stabilized nickel(0) nanoclusters as catalyst,” *Int. J. Hydrogen Energy*, vol. 32, no. 12, pp. 1707–1715, Aug. 2007.

[41] W. Ye, H. Zhang, D. Xu, L. Ma, and B. Yi, “Hydrogen generation utilizing alkaline sodium borohydride solution and supported cobalt catalyst,” *J. Power Sources*, vol. 164, no. 2, pp. 544–548, Feb. 2007.

[42] U. B. Demirci and F. Garin, “Promoted sulphated-zirconia catalysed hydrolysis of sodium tetrahydroborate,” *Catal. Commun.*, vol. 9, no. 6, pp. 1167–1172, Mar. 2008.

[43] D. Xu, H. Zhang, and W. Ye, “Hydrogen generation from hydrolysis of alkaline sodium borohydride solution using Pt/C catalyst,” *Catal. Commun.*, vol. 8, no. 11, pp. 1767–1771, Nov. 2007.

[44] C. Wu, H. Zhang, and B. Yi, “Hydrogen generation from catalytic hydrolysis of sodium borohydride for proton exchange membrane fuel cells,” *Catal. Today*, vol. 93–95, pp. 477–483, Sep. 2004.

[45] Y. Kojima, K. Suzuki, K. Fukumoto, M. Sasaki, T. Yamamoto, Y. Kawai, and H. Hayashi, “Hydrogen generation using sodium borohydride solution and metal catalyst coated on metal oxide,” *Int. J. Hydrogen Energy*, vol. 27, no. 10, pp. 1029–1034, Oct. 2002.

[46] Y. Kojima, K. Suzuki, K. Fukumoto, Y. Kawai, M. Kimbara, H. Nakanishi, and S. Matsumoto, “Development of 10 kW-scale hydrogen generator using chemical hydride,” *J. Power Sources*, vol. 125, no. 1, pp. 22–26, Jan. 2004.

[47] P. Krishnan, T.-H. Yang, W.-Y. Lee, and C.-S. Kim, “PtRu-LiCoO2—an efficient catalyst for hydrogen generation from sodium borohydride solutions,” *J. Power Sources*, vol. 143, no. 1–2, pp. 17–23, Apr. 2005.

[48] P. Krishnan, K.-L. Hsueh, and S.-D. Yim, “Catalysts for the hydrolysis of aqueous borohydride solutions to produce hydrogen for PEM fuel cells,” *Appl. Catal. B Environ.*, vol. 77, no. 1–2, pp. 206–214, Nov. 2007.

[49] U. B. Demirci and F. Garin, “Ru-based bimetallic alloys for hydrogen generation by hydrolysis of sodium tetrahydroborate,” *J. Alloys Compd.*, vol. 463, no. 1–2, pp. 107–111, Sep. 2008.

[50] V. I. Simagina, P. a. Storozhenko, O. V. Netskina, O. V. Komova, G. V. Odegova, T. Y. Samoilenko, and a. G. Gentsler, “Effect of the nature of the active component and support on the activity of catalysts for the hydrolysis of sodium borohydride,” *Kinet. Catal.*, vol. 48, no. 1, pp. 168–175, Feb. 2007.

[51] O. V. Komova, V. I. Simagina, O. V. Netskina, D. G. Kellerman, A. V. Ishchenko, and N. a. Rudina, “LiCoO2-based catalysts for generation of hydrogen gas from sodium borohydride solutions,” *Catal. Today*, vol. 138, no. 3–4, pp. 260–265, Nov. 2008.

[52] B. S. Richardson, J. F. Birdwell, F. G. Pin, J. F. Jansen, and R. F. Lind, “Sodium borohydride based hybrid power system,” *J. Power Sources*, vol. 145, no. 1, pp. 21–29, Jul. 2005.

[53] R. Oronzio, G. Monteleone, A. Pozio, M. De Francesco, and S. Galli, “New reactor design for catalytic sodium borohydride hydrolysis,” *Int. J. Hydrogen Energy*, vol. 34, no. 10, pp. 4555–4560, May 2009.

[54] J. S. Zhang, W. N. Delgass, T. S. Fisher, and J. P. Gore, “Kinetics of Ru-catalyzed sodium borohydride hydrolysis,” *J. Power Sources*, vol. 164, no. 2, pp. 772–781, Feb. 2007.

[55] A. Hung, S. Tsai, Y. Hsu, J. Ku, Y. Chen, and C. Yu, “Kinetics of sodium borohydride hydrolysis reaction for hydrogen generation,” *Int. J. Hydrogen Energy*, vol. 33, no. 21, pp. 6205–6215, Nov. 2008.

[56] J. Park, P. Shakkthivel, H. Kim, M. Han, J. Jang, Y. Kim, and Y. Shul, “Investigation of metal alloy catalyst for hydrogen release from sodium borohydride for polymer electrolyte membrane fuel cell application,” *Int. J. Hydrogen Energy*, vol. 33, no. 7, pp. 1845–1852, Apr. 2008.

[57] S. C. Amendola, S. L. Sharp-Goldman, M. S. Janjua, M. T. Kelly, P. J. Petillo, and M. Binder, “An ultrasafe hydrogen generator: aqueous, alkaline borohydride solutions and Ru catalyst,” *J. Power Sources*, vol. 85, no. 2, pp. 186–189, Feb. 2000.

[58] C.-L. Hsueh, C.-Y. Chen, J.-R. Ku, S.-F. Tsai, Y.-Y. Hsu, F. Tsau, and M.-S. Jeng, “Simple and fast fabrication of polymer template-Ru composite as a catalyst for hydrogen generation from alkaline NaBH4 solution,” *J. Power Sources*, vol. 177, no. 2, pp. 485–492, Mar. 2008.

[59] A. M. F. R. Pinto, M. J. F. Ferreira, V. R. Fernandes, and C. M. Rangel, “Durability and reutilization capabilities of a Ni–Ru catalyst for the hydrolysis of sodium borohydride in batch reactors,” *Catal. Today*, vol. 170, no. 1, pp. 40–49, Jul. 2011.

[60] F. Barbir, *PEM Fuel Cells: Theory and Practice*, First Edit. Elsevier Academic Press, 2005, p. 456.

[61] K. Sopian and W. R. Wan Daud, "Challenges and future developments in proton exchange membrane fuel cells," *Renew. Energy*, vol. 31, no. 5, pp. 719–727, Apr. 2006.

[62] G. Hoogers, *Fuel Cell Technology Handbook*. CRC Press LLC, 2003.

[63] "Cool Electric Car," 2006. [Online]. Available: http://www.mycoolelectriccar.com/hydrogen-fuel-cells.html. [Accessed: 26-Jan-2014].

[64] J. Larminie and A. Dicks, *Fuel cell systems explained*, 2nd ed. West Sussex: John Wiley & Sons Ltd, 2003, p. 418.

[65] Universidade dos Açores, "Laboratório de ambiente marinho e tecnologia." [Online]. Available: http://www.lamtec-id.com/energias/hidrogenio.php. [Accessed: 27-Jan-2014].

[66] L. Dinis and P. Ribeiro, "Cap.6 - Cascas axissimétricas: teoria de membrana." Disciplina de Placas e Cascas, 5º ano do MIEM, FEUP, p. 47, 2012.

[67] A. Zingoni, "Stresses and deformations in egg-shaped sludge digestors: membrane effects," *Eng. Struct.*, vol. 23, no. 11, pp. 1365–1372, Nov. 2001.

[68] E. Ventsel and T. Krauthammer, *Thin Plates and Shells: Theory: Analysis, and Applications*. Marcel Dekker, Inc., 2001, p. 688.

[69] "HySafe - Safety of Hydrogen as an Energy Carrier," 2007. [Online]. Available: http://www.hysafe.org/. [Accessed: 24-Jan-2014].

[70] L. S. K., K. H. S., N. S. J., and H. J. H., "Hydrogen Permeability, Diffusivity, and Solubility of SUS 316L Stainless Steel in the Temperature Range 400 to 800 ℃ for Fusion Reactor Applications," *J. Korean Phys. Soc.*, vol. 59, no. 5, p. 3019, Nov. 2011.

[71] E. Owczarek and T. Zakroczymski, "Hydrogen transport in a duplex stainless steel," *Acta Mater.*, vol. 48, no. 12, pp. 3059–3070, Jul. 2000.

[72] A. Barnoush, "Hydrogen embrittlement." p. 61, 2011.

[73] S. L. Robinson, B. P. Somerday, and N. R. Moody, "Hydrogen embrittlement of stainless steels," 2004, p. 6.

[74] E. Herms, J. . Olive, and M. Puiggali, "Hydrogen embrittlement of 316L type stainless steel," *Mater. Sci. Eng. A*, vol. 272, no. 2, pp. 279–283, Nov. 1999.

[75] Y. Kojima, Y. Kawai, H. Nakanishi, and S. Matsumoto, "Compressed hydrogen generation using chemical hydride," *J. Power Sources*, vol. 135, no. 1–2, pp. 36–41, Sep. 2004.

Appendix A| Reactor thickness calculations

Table 11| Thickness calculations for the top of egg-shaped mini-reactor.

TOP				
r_t=	4.5	mm		
φ_{ot} =	58.61	°	1.023	rad
r_t (1-cos(φ_{ot}) =	2.156	mm		
0	≤ φ_t ° ≤	58.61		
φ_t =	58.61	°	1.023	rad
$N_{\varphi t}$ =	1.91×10^{-3}	N mm^{-1}		
$N_{\theta t}$ =	6.64×10^{-3}	N mm^{-1}		

VON MISES CRITERION			
$h\times\sigma_\theta$ =	N_θ =	6.64×10^{-3}	N mm^{-1}
$h\times\sigma_\varphi$ =	N_φ =	1.91×10^{-3}	N mm^{-1}
σ_v^2 =	$\sigma_\theta^2 - \sigma_\theta\times\sigma_\varphi + \sigma_\varphi^2$		
$h^2\times\sigma_v^2$ =	$N_\theta^2 - N_\theta\times N_\varphi + N_\varphi^2$ =	3.50×10^{-5}	(N mm^{-1})^2
$\sigma_v^2 = \sigma_y^2$	h =	1.02×10^{-5}	mm

Table 12| Thickness calculations for the bottom of egg-shaped mini-reactor.

BOTTOM				
r_b =	10	mm		
φ_{ob} =	82.58	°	1.441	rad
r_b (1-cos(φ_{ob}) =	8.708	mm		
82.58	≤ φ_b ° ≤	180		
φ_b =	179	°	3.124	rad
c_2 =	2.88			
$N_{\varphi b}$ =	6.03×10^{2}	N mm^{-1}		
$N_{\theta b}$ =	-6.03×10^{2}	N mm^{-1}		

VON MISES CRITERION			
$h\times\sigma_\theta$ =	N_θ =	-6.03×10^{2}	N mm^{-1}
$h\times\sigma_\varphi$ =	N_φ =	6.03×10^{2}	N mm^{-1}
σ_v^2 =	$\sigma_\theta^2 - \sigma_\theta\times\sigma_\varphi + \sigma_\varphi^2$		
$h^2\times\sigma_v^2$ =	$N_\theta^2 - N_\theta\times N_\varphi + N_\varphi^2$ =	1.09×10^{6}	(N mm^{-1})^2
$\sigma_v^2 = \sigma_y^2$	h =	1.80	mm

Table 13| Thickness calculations for the middle zone of egg-shaped mini-reactor.

MIDDLE				
R_c =	37.5	mm		
A =	27.7	mm		
$R_c \times \cos(\varphi_{ot})$ =	19.5	mm		
$R_c \times \cos(\varphi_{ob})$ =	4.8	mm		
58,61	≤ φ_m ° ≤	82.58		
φ_m =	82.58	°	1.441	rad
c_1 =	-5.40			
$N_{\varphi m}$ =	8.38×10^{-1}	N mm^{-1}		
$N_{\theta m}$ =	-7.20×10^{-2}	N mm^{-1}		

VON MISES CRITERION			
$h \times \sigma_\theta$ =	N_θ =	-7.20×10^{-2}	N mm^{-1}
$h \times \sigma_\varphi$ =	N_φ =	8.38×10^{-1}	N mm^{-1}
σ_v^2 =	$\sigma_\theta^2 - \sigma_\theta \times \sigma_\varphi + \sigma_\varphi^2$		
$h^2 \times \sigma_v^2$ =	$N_\theta^2 - N_\theta \times N_\varphi + N_\varphi^2$ =	7.68×10-1	(N mm^{-1})^2
$\sigma_v^2 = \sigma_y^2$	h =	1.51×10^{-3}	mm

Appendix B| Novel mini-reactor blueprint

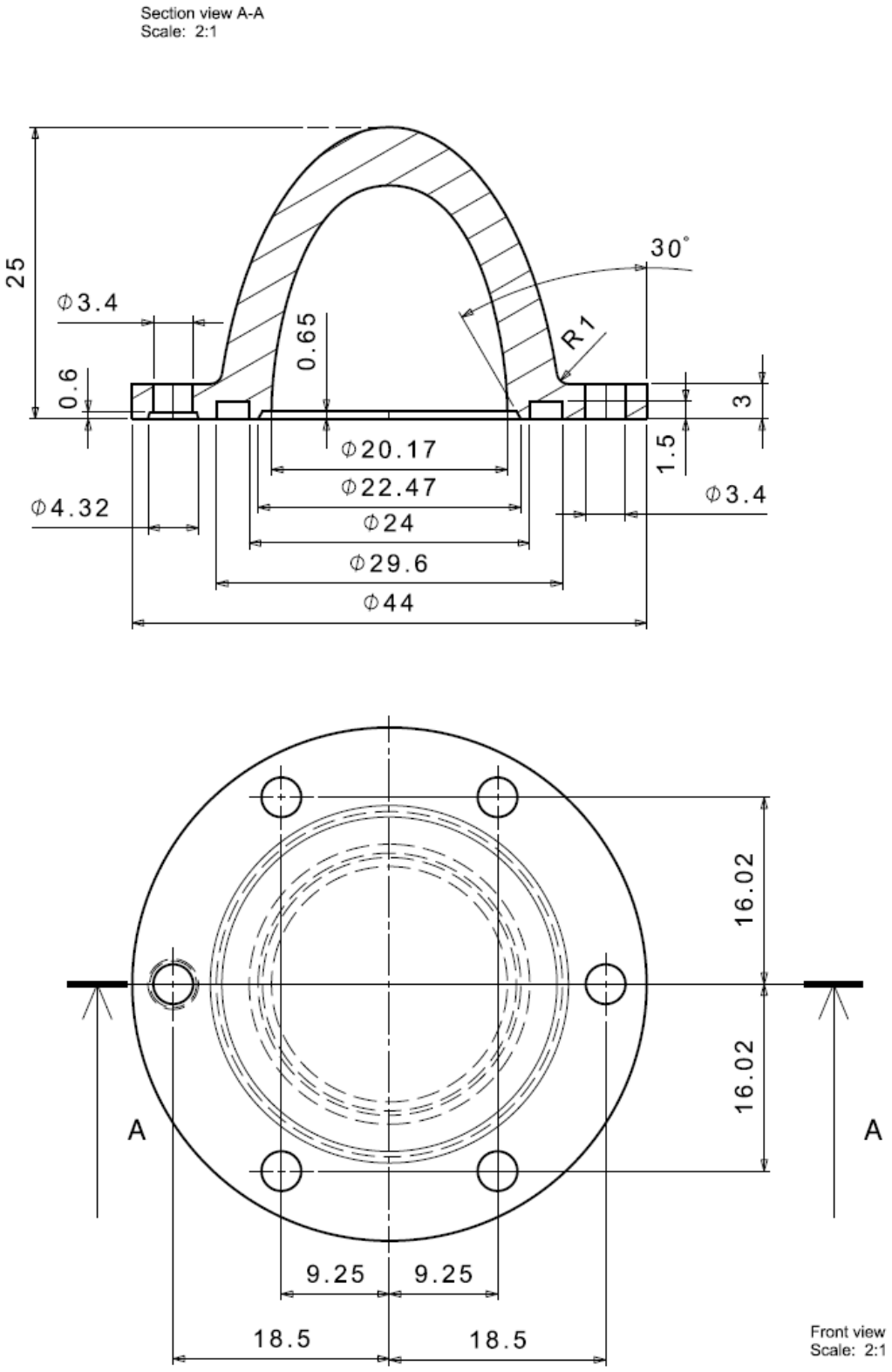

Figure 33| Novel mini-reactor blueprint: top view.

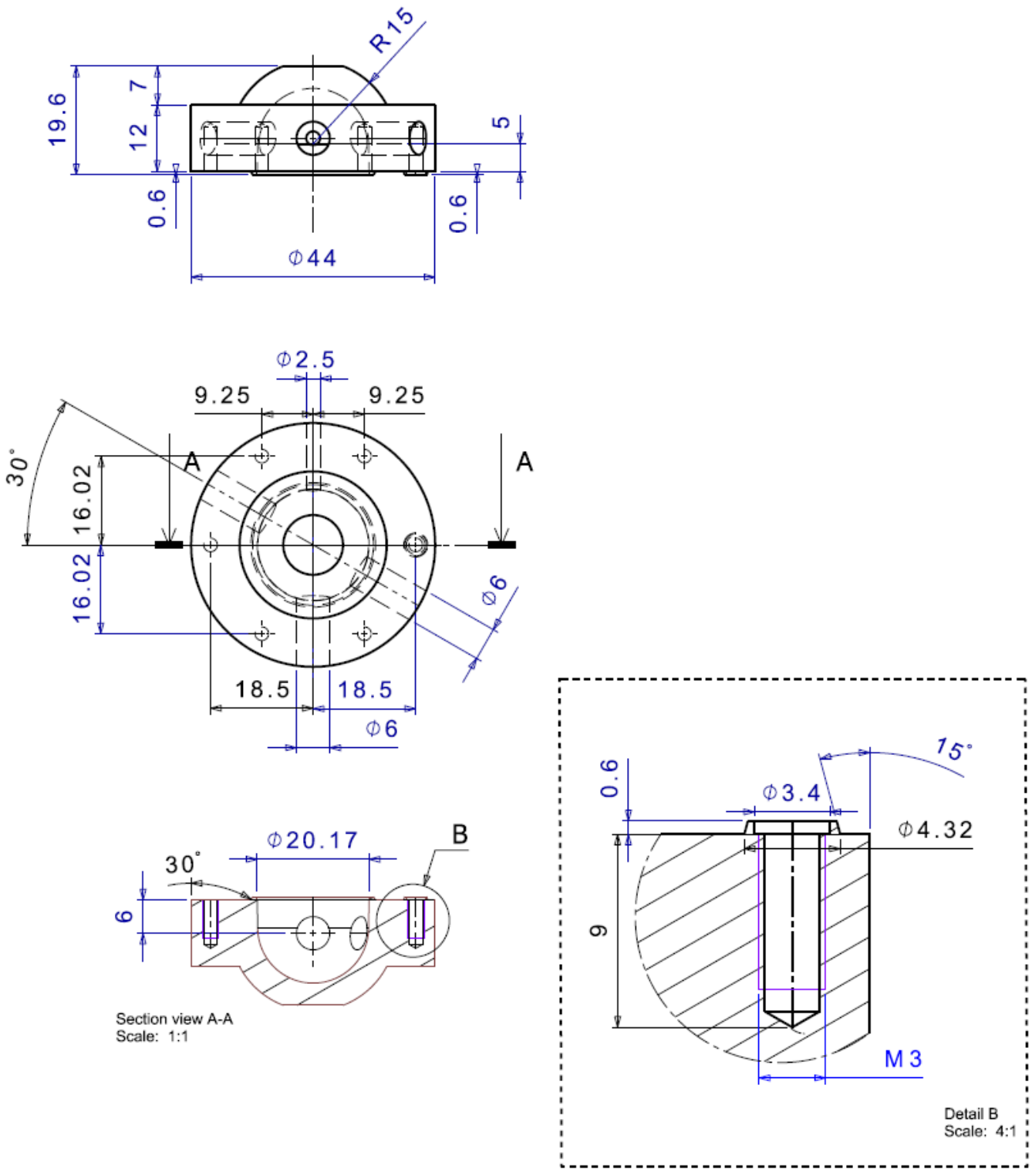

Figure 34| Novel mini-reactor blueprint: bottom view.